Journal of Environmental Radioactivity 157 (2016) 113–130

Contents lists available at ScienceDirect

Journal of Environmental Radioactivity

journal homepage: www.elsevier.com/locate/jenvrad

Review

Fukushima Daiichi Nuclear Plant accident: Atmospheric and oceanic impacts over the five years

Katsumi Hirose

Department of Materials and Life Sciences, Sophia University, Tokyo, Japan

ARTICLE INFO

Article history:
Received 21 January 2016
Accepted 21 January 2016
Available online 28 March 2016

Keywords:
Fukushima Daiichi Nuclear Power Plant
Atmosphere
Deposition
Ocean
Dispersion
^{137}Cs
^{131}I
Numerical model
Source term

ABSTRACT

The Fukushima Daiichi Nuclear Plant (FDNPP) accident resulted in huge environmental and socioeconomic impacts to Japan. To document the actual environmental and socioeconomic effects of the FDNPP accident, we describe here atmospheric and marine contamination due to radionuclides released from the FDNPP accident using papers published during past five years, in which temporal and spatial variations of FDNPP-derived radionuclides in air, deposition and seawater and their mapping are recorded by local, regional and global monitoring activities. High radioactivity-contaminated area in land were formed by the dispersion of the radioactive cloud and precipitation, depending on land topography and local meteorological conditions, whereas extremely high concentrations of ^{131}I and radiocesium in seawater occurred due to direct release of radioactivity-contaminated stagnant water in addition to atmospheric deposition. For both of atmosphere and ocean, numerical model simulations, including local, regional and global-scale modeling, were extensively employed to evaluate source terms of the FDNPP-derived radionuclides from the monitoring data. These models also provided predictions of the dispersion and high deposition areas of the FDNPP-derived radionuclides. However, there are significant differences between the observed and simulated values. Then, the monitoring data would give a good opportunity to improve numerical modeling.

Contents

1. Introduction

In March 11, 2011, a 9.0-magnitude earthquake occurred near northeast Honshu, Japan, creating a devastating tsunami. The

E-mail address: hirose45037@mail2.accsnet.ne.jp.

http://dx.doi.org/10.1016/j.jenvrad.2016.01.011
0265-931X/

earthquake and subsequent tsunami, which flooded over 500 km^2 of land, resulted in the loss of about 20 000 lives and destroyed property, infrastructure and natural resources. The loss of off-site and on-site electrical power (station blackout) and compromised safety systems at the Fukushima Daiichi Nuclear Power Plant (FDNPP) led to severe core damage to three of the six nuclear reactors on the site. As a result, large amounts of radioactivity were released in the environment from the FDNPP. The FDNPP accident, which has been rated on the International Atomic Energy Agency (IAEA) International Nuclear and Radiological Event Scale (INES) as a "Major Accident" as INES 7 as did the Chernobyl accident, was one of the biggest environmental disasters in recent years. In order to implement adequate protective actions and to assess the environmental impact of the FDNPP radioactivity, a lot of environmental monitoring has been conducted by the national government, local governments, research institutes and universities in Japan and world including the CTBTO network. Maps of deposition densities of FDNPP-derived ^{137}Cs, obtained by areal monitoring, are shown in Fig. 1. The environmental contamination of the FDNPP-derived radionuclides is characterized by complicated land topography in addition to the FDNPP location on the North Pacific west coast. In contrast of the Chernobyl accident, therefore, marine radioactivity monitoring is important. The environmental monitoring of land revealed that heavy radioactivity-contaminated area spread to about 60 km northwest the FDNPP (Yoshida and Takahashi, 2012), where deposition is controlled by land topography and meteorological factors.

The FDNPP-derived radionuclides spread around the world. The marine environment was severely contaminated by atmospheric deposition and direct discharge of highly radioactivity-contaminated stagnant water. Many kinds of radionuclides were released in the atmospheric and marine environment; the dominant released radionuclides were gaseous and volatile elements such as ^{133}Xe, ^{131}I, ^{134}Cs and ^{137}Cs. In initial stages of the accident, short-lived γ-emitters such as ^{133}I, ^{132}I, ^{136}Cs, ^{132}Te, ^{129m}Te (^{129}Te), ^{99}Mo(^{99m}Tc), ^{140}Ba(^{140}La), ^{95}Nb and ^{110m}Ag were observed in environmental samples. Furthermore, long-lived radionuclides such as ^{89}Sr, ^{90}Sr, U isotopes (Sakaguchi et al., 2014), Pu isotopes (Yamamoto et al., 2014; Zheng et al., 2012), ^{241}Am, Cm isotopes (Yamamoto et al., 2014) and ^{129}I (Miyake et al., 2012) were observed as minor nuclides.

During the past five years from the FDNPP accident, many papers related to the FDNPP accident have been published, in which some review articles (Koo et al., 2014; Thakur et al., 2013) such as comparison between the Chernobyl and FDNPP accidents (Steinhauser et al., 2014) and books (Povinec et al., 2013a; UNSCEAR, 2013; Nakata and Sugisaki, 2015) are included. Most of the papers regarding atmospheric monitoring data have been published in 2011–2012. After that, however, important monitoring data related to initial stage of the FDNPP accident were recorded (Tsuruta et al., 2014). For the FDNPP accident, atmospheric dispersion models have been employed from the initial stage of the

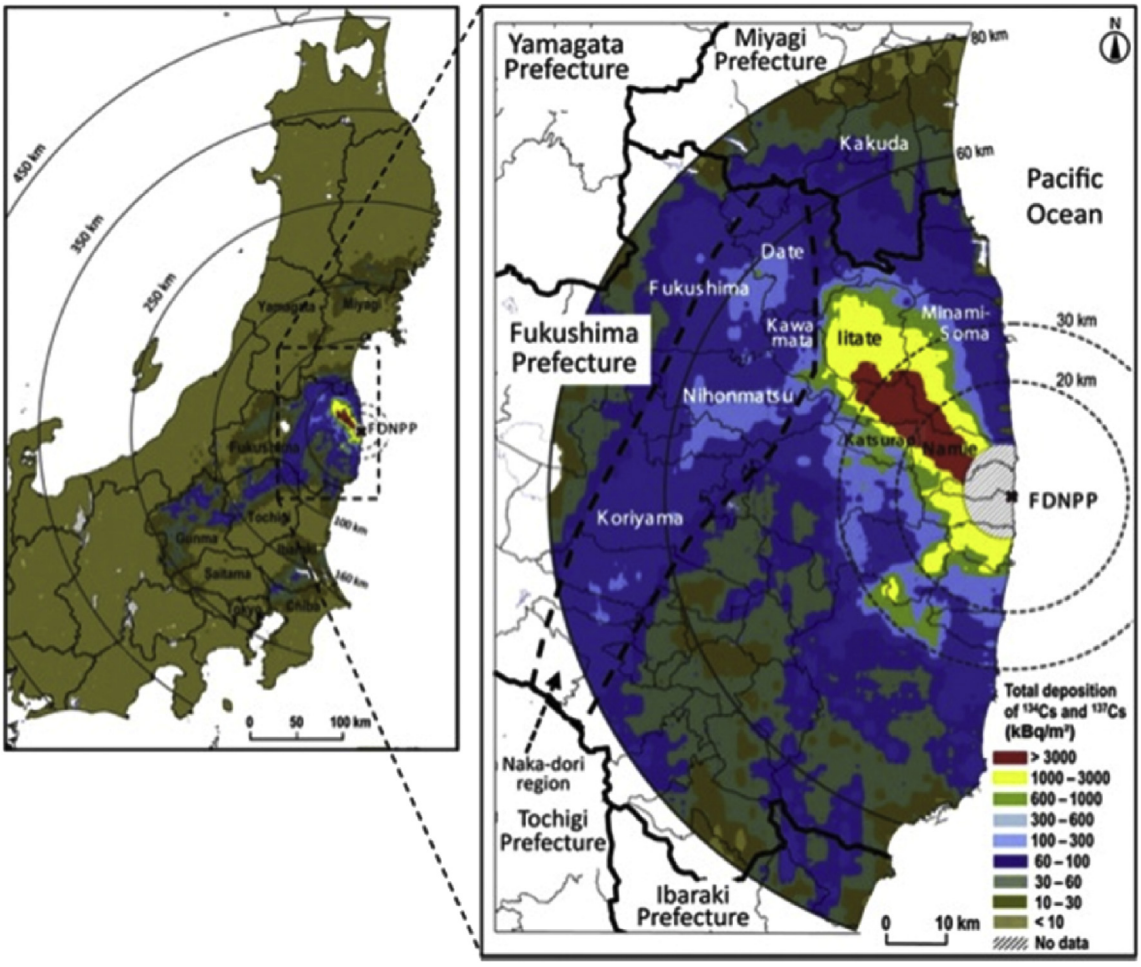

Fig. 1. The geographical distribution of the total deposition of the FDNPP-derived radiocesium (^{134}Cs + ^{137}Cs) in the northeast Honshu Island, Japan. The total radiocesium (^{134}Cs + ^{137}Cs) deposition was estimated by gamma-ray measurements using aircraft in the northeast Honshu Island, especially, Fukushima Prefecture.

accident in order to do adequate protective actions and to have source terms of the atmospheric emission of the FDNPP-derived radionuclides. In order to improve the atmospheric dispersion model, comparison exercises between models have been carried out (SCJ, 2014; Draxler et al., 2015). Although the major atmospheric radionuclide release due to the accident ceased by the end of April 2011, post-accident atmospheric emission, which were occurred by natural processes such as resuspension of deposited radionuclides and anthropogenic activities including mediation processes of damaged reactors, have been monitored within 300 km from the FDNPP (Hirose, 2013, 2015a; Igarashi et al., 2015; Stainhauser et al., 2015).

Marine radioactivity monitoring started just after the FDNPP accident. After discover of direct release of radioactivity-contaminated water in early April 2011, monitoring was strengthened (Povinec et al., 2013). However, marine monitoring data are fewer than those on land due to limited ship resources. Source terms, the atmospheric deposition and direct release, are important to assess effects of the FDNPP-derived radionuclides to marine environment. Development of the ocean circulation model allows us to have better estimates of source terms of the direct release from the monitoring data (Tsumune et al., 2012). The model simulations can predict dispersion and transport of the FDNPP-derived radionuclides in the North Pacific (Nakano and Povinec, 2012; Behrens et al., 2012), although its verification is a further issue. In order to improve the ocean dispersion model, comparison exercises between models have been carried out (Masumoto et al., 2012).

In this review paper, we describe actual situations of atmospheric and oceanic contamination of the FDNPP-derived radionuclides by using research papers published past five years. The FDNPP accident resulted in socioeconomic impacts, as did environmental impacts. We also describe shortly socioeconomic impacts due to the FDNPP accident.

2. Atmospheric impact of FDNPP-derived radioactivity

2.1. Air concentrations

Radioactivity measurement in surface air is one of the most important issues in emergency environmental monitoring. Air monitoring activities in Japan, in which Japanese Government, TEPCO, local governments, national research institutes and university have conducted air sampling in different areas, intensified after the FDNPP accident. TEPCO focused in the FDNPP site, and JAEA monitored in the area from 20 km to 60 km of the FDNPP using monitoring car (Povinec et al., 2013a). Major air continuous monitoring was conducted in the Kanto area (Furuta et al., 2011; Yonezawa and Yamamoto, 2011; Amano et al., 2012; Haba et al., 2012; Kanai, 2012; Doi et al., 2013), whereas in the region further from the FDNPP, a limited air radioactivity measurement has been carried out (Momoshima et al., 2012). On the site, the highest total ^{131}I concentration in surface air (5.94 kBq m^{-3}) occurred on 19 March 2011, whereas the highest total ^{137}Cs concentration in surface air (430 Bq m^{-3}) was observed on 25 March 2011. Tsuruta et al. (2014) realized detailed features of FDNPP-derived ^{137}Cs in surface air of Fukushima and Kanto area by analyzing filter-tapes of operational air pollution monitoring stations, in which time series of ^{137}Cs concentrations in surface air were obtained during the period of March 12–23, 2011 just after the FDNPP accident. Four ^{137}Cs peaks were observed at Minami-soma sites about 40 km north FDNPP (first peak: Mar. 12–13, 577 Bq m^{-3} (1 h mean value); second peak: Mar. 15–16, 21 Bq m^{-3}; third peak: Mar. 18–19, 430 Bq m^{-3}; fourth peak: Mar. 20–21, 360 Bq m^{-3}), whereas two ^{137}Cs peaks occurred in the central area of Fukushima prefecture and Kanto plain (first peak: Mar. 15–16, 330 Bq m^{-3} (central Fukushima), 175 Bq m^{-3} (Kanto Plain); second peak: Mar. 20–21, 81 Bq m^{-3} (central Fukushima), 309 Bq m^{-3} (Kanto Plain)). Surface air measurements as shown in Fig. 2 documented that radioactive plume first arrived in Kanto plain on 15 March 2011; the first peak of ^{131}I, being maximum concentrations at Tsukuba (33 Bq m^{-3} (8 h mean value)) (Doi et al., 2013) and Oarai (1.4 × 10^3 Bq m^{-3} (3 h mean value)) (Furuta et al., 2011) during the observation period, respectively, and the high ^{134}Cs and ^{137}Cs concentrations in surface air were observed in Oarai, Tsukuba, Wako and Inage, where the ^{137}Cs concentrations in surface air were 1.9 × 10^2 Bq m^{-3} (3 h mean value) (Furuta et al., 2011), 3.8 Bq m^{-3} (3 h mean value) (Doi et al., 2013), 8.8 Bq m^{-3} (0.5 h mean value) and 0.87 Bq m^{-3} (27 h mean value) (Amano et al., 2012), respectively. After the first peak, the second peak of the FDNPP-derived radionuclide concentrations in surface air at Oarai, Tsukuba and Inage occurred, which were 160 Bq m^{-3} (9 h mean value), 4.6 Bq m^{-3} (48 h mean value) and 6.1 Bq m^{-3} (26 h mean value), respectively. The third peak of the surface ^{137}Cs in Kanto Plain appeared in March 29–31. The observed third peak concentrations of ^{137}Cs in surface air at Oarai, Tsukuba and Inage were 3.2 Bq m^{-3} (12 h mean value), 0.23 Bq m^{-3} (48 h mean value) and 0.69 Bq m^{-3} (24 h mean value), respectively. After that, the surface ^{137}Cs in the Kanto Plain decreased rapidly and reached about 0.1 mBq m^{-3} in June 2011 (Kanai et al., 2013). However, decrease rate of the surface ^{137}Cs slowed down and was still higher than pre-accident level until the end of 2012.

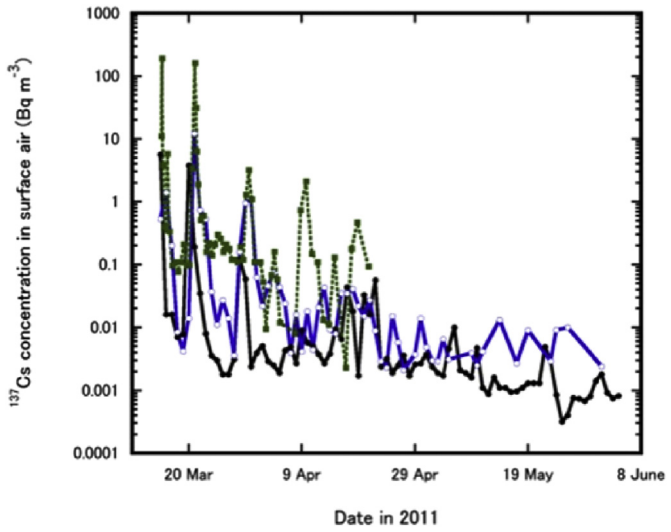

Fig. 2. Temporal variations of ^{137}Cs concentrations in surface air observed in Kanto area. Blue line: Tsukuba, green line: Oarai, black line: Inage. Referred from Povinec et al., 2013. (For interpretation of the references to color in this figure legend, the reader is referred to the web version of this article.)

The concentrations of the FDNPP-derived radionuclides in surface air were determined in the regions further from the FDNPP (Momoshima et al., 2012), which included Fukuoka (32°27′N, 130°25′E, 1050 km west of the FDNPP) and Matsue (35°28′N, 133°3′E, 750 km west of the FDNPP) (Povinec et al., 2013a). For the western remote sites, ^{131}I was first detected in dust samples on March 17, 2011 at Fukuoka, although its level was very low (0.036 mBq m^{-3}) in contrast of the stations in Kanto Plain. At Fukuoka and Matsue, the ^{131}I concentrations in surface air exponentially increased and reached a maximum on April 6. After occurrence of a first peak, the ^{131}I concentration in surface air decreased. On April 20, a weak second peak of the surface ^{131}I occurred, in which the second peak was more remarkable at Matsue. After that, the ^{131}I concentration decreased and was less than detection limit until end of April. Cesium-137 was first detected in

dust samples on March 29, 2011 at Fukuoka, although its level was very low (0.027 mBq m^{-3}) as did ^{131}I. At Fukuoka, the ^{137}Cs concentrations in surface air rapidly increased and reached a maximum on April 6, when it coincided with the maximum of ^{131}I. After occurrence of a peak, the ^{137}Cs concentration in surface air in Fukuoka decreased and was less than the detection limit until end of April, whereas a marked second peak appeared on April 20.

Air monitoring activity was intensified across the northern hemisphere following the first reports of atmospheric releases from Japan. The Comprehensive Nuclear-Test-Ban Treaty (CTBT) was adopted by the United Nations General Assembly on September 10, 1996 (CTBT). Within the CTBT the International Monitoring System (IMS) was defined to monitor the world for nuclear explosions. The IMS comprises four primary monitoring technologies: radionuclide, seismic, hydroacustic and infrasound. The FDNPP-derived radionuclides were first determined by the global CTBTO network. Thakur et al. (2013) reported overview of surface air concentrations of the FDNPP-derived radionuclides obtained from the world monitoring network. Dominant FDNPP-derived radionuclides (^{133}Xe, ^{131}I, ^{134}Cs and ^{137}Cs) in surface air of the North America (Canada and US) were first detected in March 17–19, 2011 (Biegalski et al., 2012; Bowyer et al., 2011; US-EPA, 2011; McNaughton, 2011; Zhang et al., 2011; MacMullin et al., 2012; Kitto et al., 2013; Miley et al., 2013). The peak concentrations of ^{131}I in air were observed in March 20–21 (Pacific Islands), March 19–April 4 (Canada), March 21–25 (Alaska), March 17–April 2 (US mainland). For many stations, occurrence of the peak ^{137}Cs and ^{134}Cs coincided with that of the peak ^{131}I, although in some stations it was delayed 1–3 days. The peak ^{131}I activity concentrations in air of Pacific Islands, Canada, Alaska, and US Mainland were in the ranges from 2.3 to 22 mBq m^{-3}, from 2.3 to 9.8 mBq m^{-3}, from 2.1 to 26 mBq m^{-3}, from 0.4 to 31 mBq m^{-3}, respectively. The peak ^{137}Cs activity concentrations in air of Canada, Alaska, and US Mainland were in the ranges from 0.35 to 4.4 mBq m^{-3}, from 0.27 to 0.92 mBq m^{-3}, from 0.23 to 9.8 mBq m^{-3}, from 0.75 to 1.9 mBq m^{-3}, respectively. After the occurrence of peak activity, the air concentration of the FDNPP-derived radionuclides decreased to the detection limits by the end of April. After traveling over the United States from west to east, the modeled transport (Takemura et al., 2011) showed that the initial contact in Europe was in the northern part of Scandinavia (IRSA data, NRPA data) and UK (Beresford et al., 2012) between March 19–20 and subsequently in most other European countries by March 23–24, 2011(Cosma et al., 2011; Lozano et al., 2011; Masson et al., 2011; Manolopoulou et al., 2011; Parache et al., 2011; Pittauerová et al., 2011; Baeza et al., 2012; Barsanti et al., 2012; Bikit et al., 2012; Carvalho et al., 2012; Clemenza et al., 2012; Evrard et al., 2012; Garcia and Garcia Ferro, 2012; Kritidis et al., 2012; Loaiza et al., 2012; Lujanienė et al., 2012; Nikolic et al., 2012; Pham et al., 2012; Povinec et al., 2012b; Rizzo and Tomarchio, 2012; De Vismes Ott et al., 2013; Glavic-Cindro et al., 2013). A measurable concentration of Fukushima radionuclides was detected in air over Europe for about 2–3 weeks. Two ^{131}I peaks were also observed in Europe. The first ^{131}I peaked around March 28–30 in the western and central Europe and the second peak was recorded around April 3–5, 2011 in the Republic of Belarus. The peak ^{131}I activity concentrations in north Europe (Scandinavia region), western central Europe, eastern central Europe and south Europe were in the ranges from 0.61 to 2.8 mBq m^{-3}, from 0.24 to 5.6 mBq m^{-3}, from 0.2 to 5.8 mBq m^{-3}, and from 0.29 to 9.6 mBq m^{-3}, respectively. The peak ^{137}Cs activity concentrations in north Europe (Scandinavia region), western central Europe, eastern central Europe and south Europe were in the ranges from 0.15 to 0.55 mBq m^{-3}, from non-detectable (ND) to 0.73 mBq m^{-3}, from ND to 0.19 mBq m^{-3}, and from ND to 1.0 mBq m^{-3}, respectively. In Arctic, particle-bound ^{131}I was first detected at Mt. Zeppelin (78° 58′N, 11° 53′E) from a sample collected between 25 March 2011 10:11 UTC and 28 March 2011 13:04UTC (Paatero et al., 2012). In contrast to North America and Europe, the FDNPP-derived radioactive cloud was transported in the Southeast Asia by northeast wind flow (Huh et al., 2012; Kim et al., 2012). The contaminated air mass first reached the Philippines and was detected on March 23, 2011, but was not detected in Vietnam. Fission products were first detected in Okinawa on March 24, Taiwan on March 25, Vietnam (Long et al., 2012) and Hong Kong (Huh et al., 2012) on March 27, South Korea on March 28 (Kim et al., 2012), on March 31 China mainland (MEP data), and the Tibet plateau on April 02, 2011 (Hsu et al., 2012). The progressive arrival of Fukushima air mass in the southwestern direction is supported by the model simulation and is consistent with transport via northeastern monsoon winds (Huh et al., 2012). Peak ^{131}I concentrations in surface air of Korea and north China, whose range was from 0.69 to 8.0 mBq m^{-3}, occurred on April 5–7, whereas occurrences of maximum ^{131}I air concentrations in the Southeast Asia including south China (range: 0.075–3.7 mBq m^{-3}), which were observed on March 31–April 2 and April 5–10, are more complicated. In western China, the ^{131}I peak was observed in on April 1–3 and on April 7–9. The peak ^{137}Cs occurred in the east and Southeast Asia during the period of April 5–10. The peak ^{137}Cs activity concentrations in Korea and north China and Southeast Asia were in the ranges from 0.09 to 1.25 mBq m^{-3} and from 0.023 to 0.65 mBq m^{-3}, respectively.

Isotope signature is an important tool to have better understanding of the environmental behaviors of the FDNPP-derived radionuclides. As it is well known that ^{134}Cs is not a direct fission product, ^{134}Cs is produced by neutron activation of ^{133}Cs, which is the decay product of ^{133}Xe present in nuclear reactors. $^{134}Cs/^{137}Cs$ ratios increase with burn-up time of nuclear fuel. Mutual relationships between ^{134}Cs and ^{137}Cs in surface air were examined (Amano et al., 2012; Doi et al., 2013; Haba et al., 2012; Biegalski et al., 2012). The $^{134}Cs/^{137}Cs$ activity ratio in surface air at all sites including Japanese and US stations, ranged from 0.9 to 1.2 as an average of 1.0 ± 0.1, was fairly stable over the time of observation, which coincides with that of deposition (Amano et al., 2012; Hirose, 2012).

Atmospheric behaviors of the FDNPP-derived radionuclides depend on physical and chemical properties of radionuclide-bearing particles. Particle size distributions of the FDNPP-derived radionuclide-bearing particles collected at Tsukuba were determined during the periods of April 4–11, and April 14–21, 2011 (Doi et al., 2013) and April 29–May 12 and May 12–26, 2011 (Kaneyasu et al., 2012). The activity median aerodynamic diameters (AMAD) of ^{131}I bearing particles were calculated to be 0.7 and 0.7 μm in April 4–11, 2011 and in April 14–21, 2011, respectively, whereas the AMADs of ^{134}Cs and ^{137}Cs bearing particles were 1.8 and 1.5 μm in April 4–11, 2011, and 1.0 and 1.0 μm in April 14–21, 2011, respectively. Adachi et al. (2013) revealed that FDNPP-derived radionuclides emitted during the period of March 15–16 were contained in spherical radiocesium-bearing particles (diameter: 2.6 μm), which were water less soluble than sulfate particles, by using an energy dispersive X-ray spectrometer. Measurements of the particle size distributions of radiocesium bearing particles in May (Kaneyasu et al., 2012) revealed that ^{137}Cs as did ^{134}Cs attached on submicrometer particles, typically sulfate particles. These findings suggest that the particle size of the ^{131}I bearing particles differed from those of radiocesium, which implies that the dispersion and deposition behaviors of ^{131}I differed from that of ^{134}Cs and ^{137}Cs and that the particle size of the radiocesium bearing particles varied with time. Masson et al. (2013) determined size distributions of the FDNPP-derived radionuclide-bearing particles at several places in Europe; the AMAD ranged between 0.25 and 0.71 μm for ^{137}Cs,

from 0.19 to 0.69 μm for ^{134}Cs and from 0.30 to 0.53 μm for ^{131}I, thus in the accumulation mode of the ambient aerosols (0.1–1 μm).

2.2. Wet and dry depositions

Measurements of radionuclides in daily deposition samples, which include wet and dry depositions, started on March 18 as emergency monitoring at Japanese Government monitoring stations (Povinec et al., 2013a). Daily radioactive deposition rates in 44 stations in Japan were recorded until the end of 2011. High radioactive deposition derived from the FDNPP accident occurred in wide area of Kanto Plain and South Tohoku from March 21 to 23, 2011. On the other hand, in Fukushima prefecture, there was no measurement of the daily radioactivity deposition during the period of March 2011 due to earthquake damages. The temporal changes of the daily ^{131}I and ^{137}Cs deposition rates during the period of March to April 2011 (Amano et al., 2012) revealed that the first deposition of the FDNPP-derived radionuclides in Kanto Plain appeared on March 15, which coincided with the first arrival of the radioactive plume. The first peaks of ^{131}I and ^{137}Cs in depositions, which were 2400 and 76 Bq m^{-2}, respectively, were observed at Inage (Chiba) on March 16, 2011, and the highest daily deposition rates of ^{131}I and ^{137}Cs were recorded on March 23 (^{131}I: 17 kBq m^{-2} d^{-1}, ^{137}Cs: 2.9 kBq m^{-2} d^{-1}) (Amano et al., 2012).

The daily radioactive deposition derived from the FDNPP accident was observed throughout April 2011. In May, 2011, the daily deposition rate of the FDNPP-derived radionuclides in most of the Japanese monitoring stations decreased below detection limit (except in Fukushima City, 37.75N, 140.47E, located about 60 km northwest of the FDNPP). In Fukushima City, in which the radioactivity measurement in daily deposition samples started on April 1, the daily ^{137}Cs deposition decreased from April 2011 to October 2011, although some high peaks occurred in the period of June–August 2011, which corresponded to heavy rainfall events. However, the enhanced daily ^{137}Cs deposition (100 Bq m^{-2}d^{-1}) appeared in the period of December 2011 to April 2012. The significant amount of ^{137}Cs was still detected in the daily deposition samples in June 2012 (Povinec et al., 2013a).

The Japanese monitoring network revealed spatial and temporal changes of the FDNPP-derived radionuclides in Japan. The temporal variations of the monthly ^{137}Cs depositions observed at Futaba, Hitachinaka and Tokyo are shown in Fig. 3. The highest monthly ^{137}Cs deposition (3340 kBq m^{-2}) was observed in March at Futaba (Fukushima Prefecture) about 5 km from the FDNPP (Hirose, 2013). The monthly ^{137}Cs depositions at the stations within 300 km from the FDNPP (except for the Kofu inland, 35.65°N, 138.57°E), and the Japan Sea-side sites (Niigata: 37.91°N, 139.04°E and Akita: 39.72°N, 140.10°E) were in the range from 1.1 kBq m^{-2} to 17 kBq m^{-2}, which are higher than the maximum monthly ^{137}Cs deposition (0.55 kBq m^{-2}) originating from the 1961-62 large-scale atmospheric nuclear testing fallout observed at Koenji (Tokyo) in 1963 (Hirose et al., 2008). The results reveal that the high ^{137}Cs-deposited areas, comparable to the cumulative amount of the ^{137}Cs deposition at Tokyo until mid-1960 (about 7 kBq m^{-2}), appeared within a region band from 100 to 300 km from the FDNPP. The spatial distribution of the monthly ^{137}Cs deposition on March 2011 revealed that the major deposition of the FDNPP-derived radionuclides occurred in the North Pacific coast and inland area east of Honshu Island, whereas there was less contribution of the FDNPP-derived radionuclides in the Japan Sea-side sites of the east Honshu Island. These findings suggest that the transport of the radioactive plume was strongly affected by land topography and that most of the FDNPP-derived radionuclides may have been injected into the boundary layer (about 1000 m).

For remote sites in Japan, the higher monthly ^{137}Cs deposition (0.17 Bq m^{-2}), which was one order of magnitude higher than pre-Fukushima levels (Igarashi et al., 2015), was observed on March at Fukuoka (33.51°N, 130.50°E) and Uruma (26.31°N, 127.90°E, Okinawa), located about 1050 km and 1750 km southwest from the FDNPP, respectively. Detection of ^{131}I and ^{134}Cs in the same sample revealed that the radionuclides were transported to Fukuoka and Uruma in the late March. The highest monthly deposition rates of radiocesium occurred at Fukuoka and Uruma in April 2011; the monthly ^{137}Cs depositions at Fukuoka and Uruma were 0.5 and 3.7 Bq m^{-2}, respectively, which were consistent with the temporal changes of the surface air concentrations of ^{137}Cs and ^{131}I (Momoshima et al., 2012; Kim et al., 2012). There were a few data of the deposition of the FDNPP-derived radionuclides in the northern Japan; an annual ^{137}Cs deposition at Sapporo (43.08°N 131.33°E) was about 7 Bq m^{-2}. Ramzaev et al. (2013) revealed that relatively high ^{134}Cs deposition densities of more than 100 Bq m^{-2} occurred in Shikotan and Kunashir Islands (South Kuril islands). Model simulation (Takemura et al., 2011) suggested that the FDNPP-derived radioactivity plume spread far eastern Siberia on March 24. Another model simulation (Huh et al., 2012) revealed that the FDNPP-derived radioactive plume was predominantly transported toward the southwest under phases of northern-easterly winds in the first week of April (6–7).

In April, higher monthly ^{137}Cs depositions were observed at the North Pacific side stations and East Japan inland stations, although the levels decreased markedly (Hirose, 2012). This suggests that the atmospheric emission of radionuclides from the Fukushima Daiichi NPP at least continued within April 2011 (Katata et al., 2012), although release rate dramatically decreased. On the other hand, the monthly ^{137}Cs deposition increased at southwest sites in Japan and at the Japan Sea-side sites comparing with that in March 2011, suggesting that the radioactive cloud dominantly affected north part of the Northern Hemisphere atmosphere. In May, 2011, the monthly ^{137}Cs depositions decreased until June 2011 at all of the monitoring stations of Japan with an apparent half-life of 12 d (Hirose, 2012), although higher ^{137}Cs depositions were observed within 300 km from the FDNPP. In August, the monthly ^{137}Cs

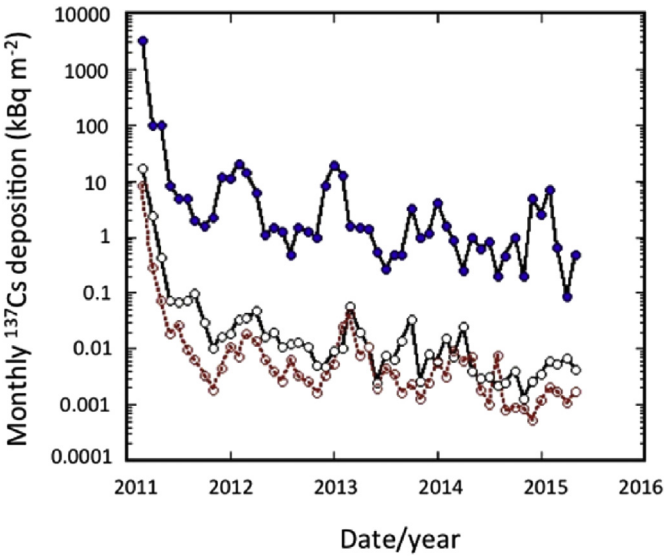

Fig. 3. Temporal variations of monthly ^{137}Cs deposition observed at Futaba (red closed square) near the FDNPP, Hitachinaka (blue open circle) and Tokyo (black closed circle). The pre-Fukushima level of the monthly ^{137}Cs deposition is the values observed in the 2000s. This figure is modified a figure referred from Hirose (2015a). (For interpretation of the references to color in this figure legend, the reader is referred to the web version of this article.)

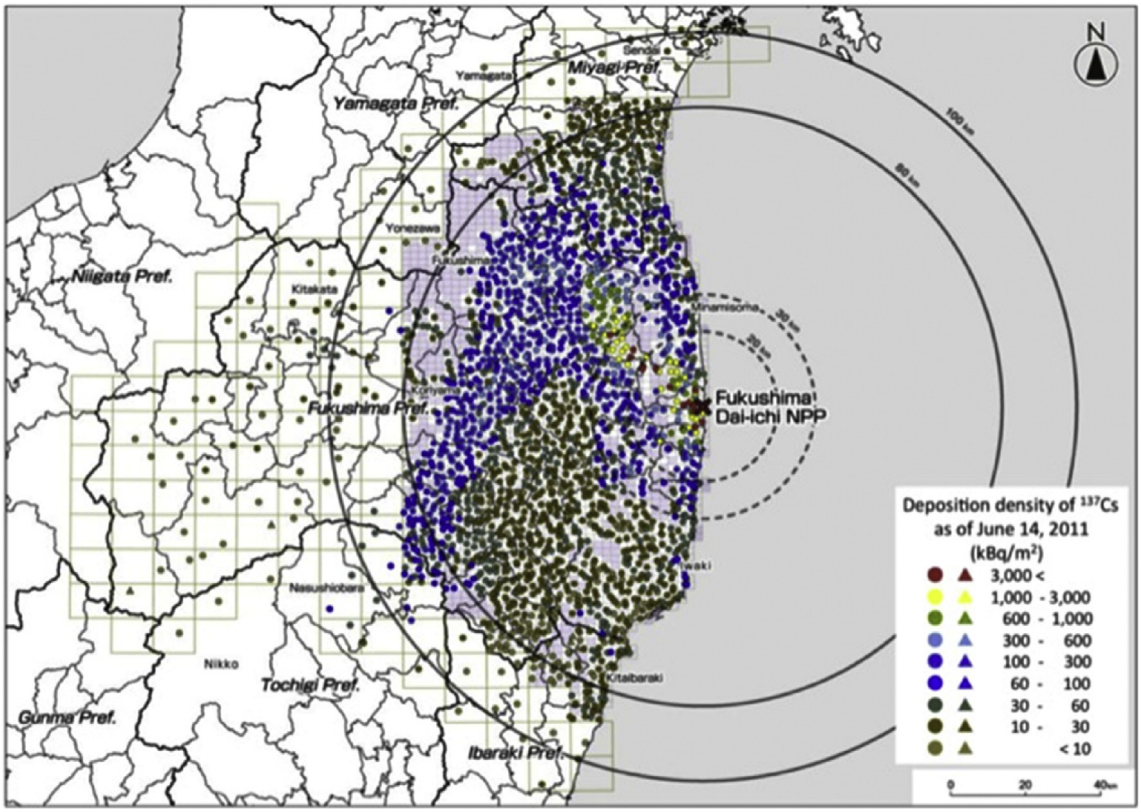

Fig. 4. Mapping of the radiocesium ($^{134}Cs + {}^{137}Cs$) deposition density estimated from measurements in soil samples in Fukushima Prefecture. Referred from Saito et al., 2015b.

depositions at many monitoring stations in southwest Japan decreased below detection limit.

The FDNPP-derived ^{137}Cs in monthly deposition samples was still measured in April 2013 at most of the monitoring stations within about 300 km of the FDNPP, in which the ^{137}Cs level until April 2013 was more than one order of magnitude higher than the pre-Fukushima level (Hirose, 2015; Igarashi et al., 2015). After 2012, the monthly ^{137}Cs deposition rates decreased at an atmospheric half-life of 1.1 years (Igarashi et al., 2015). Continuous atmospheric emission of radiocesium from the FDNPP (Hirose, 2015), resuspension of deposited ^{137}Cs on land surface (Hirose, 2013), burning of contaminated wastes including biomass are speculated as processes to support air concentrations and deposition of the FDNPP-derived ^{137}Cs since 2012.

Radioactive strontium was also released into the atmosphere due to the FDNPP accident, as observed at Tsukuba, Japan. However, the environmental impact of ^{90}Sr was small; annual ^{90}Sr deposition in 2011 was 10.6 Bq m^{-2} y^{-1}, which corresponded to only one to 2500 of annual ^{137}Cs deposition (Igarashi et al., 2015).

2.3. Mapping of the deposition density

In order to effectively conduct radiation protective actions for the FDNPP-derived radionuclide distribution, it is essential to construct detailed radioactivity contamination (deposition density) maps. Airborne monitoring is a powerful tool to depict highly radioactivity-contaminated area, as shown in Fig. 1. The early campaign of airborne monitoring, which surveyed most of the area within 30 km of the FDNPP, was conducted by the U.S. Department of Energy/National Nuclear Security Administration (US DOE/NNSA) from March 17 to 19 (Lyons and Colton, 2012). Serious deposition due to the Fukushima fallout spread about 60 km northwest from the FDNPP. The airborne monitoring of surface contamination was continued by MEXT (JAEA) with cooperation of US DOE since April 6, 2011. Relatively high deposition areas spread 300 km from the FDNPP (Fig. 1), supported by deposition data (Hirose, 2012) and model simulation (Morino et al., 2011) for the Kanto Basin. Kinoshita et al. (2011) conducted initial mapping of deposition densities of radiocesium and ^{129m}Te in central-east Japan (Ibaragi and Fukushima Prefectures), except for the evacuated area. The mapping of radioactivity-contaminated area was based on radioactivity measurements from large-scale soil sampling in Fukushima Prefecture (Onda et al., 2015; Saito et al., 2015b), and airborne monitoring using NaI (Tl) detectors placed on a helicopter (Sanada et al., 2014). Comparison between airborne monitoring data and large-scale soil data provides the most adequate conversion factors to estimate the FDNPP-derived radionuclide deposition from airborne gamma-ray measurement. The airborne monitoring and radioactivity mapping can delineate the radiocesium-contaminated area with deposition density of more than 10 kBq m^{-2}. On the other hand, contamination maps of ^{131}I, ^{129m}Te and ^{110m}Ag were created by the large-scale soil radioactivity mapping project (Saito et al., 2015b), in which mapping of the ^{131}I deposition density was incomplete due to short half-life of ^{131}I. Recently a more precise map of the ^{131}I deposition density was reconstructed using $^{129}I/^{131}I$ ratios in the FDNPP derived radionuclides and ^{129}I measurements (Miyake et al., 2012; Muramatsu et al., 2015), in which the spatial distribution of ^{131}I differed from that of radiocesium, especially, in south region of the FDNPP. The map of FDNPP-derived ^{137}Cs deposition density is shown in Fig. 4. The high radiocesium-contaminated area due to the Fukushima fallout spread narrow area northwestward from the FDNPP. Another typical future is that higher contaminated areas are present in Fukushima Basin besides northern and southern mountains, mountainside of the north Kanto Plain and the central part of the Kanto Plain. This finding suggests that the Fukushima fallout was

strongly governed by topography and geographical distribution of rainfall. In order to elucidate spatial distributions and temporal changes of the FDNPP-derived radionuclides in the Tohoku and Kanto regions, soil sampling (about 1000 locations) was conducted in March–December 2011 and led to maps of ^{134}Cs, ^{137}Cs and ^{110m}Ag deposition densities (Mikami et al., 2015). The results suggests that there is a little change of ^{134}Cs and ^{137}Cs deposition densities between March and December 2012, which means that the weathering effects, especially horizontal mobility, of radiocesium were barely observed in the overall trends.

2.4. Atmospheric dispersion model of radionuclides

For the FDNPP accident, numerical models to reproduce ambient dose rate, surface air concentrations and deposition of the FDNPP-derived radionuclides were applied to estimate the total atmospheric emission and temporal change of emission rates of the FDNPP radionuclides. The dispersion model is considered to be important to inform planning for field monitoring operations and to implement protective actions for Japanese citizens. Predictions of possible radioactive plume arrival times and dose levels at world locations, especially Japan, are the most important issue. A critical issue of application of model simulation for the FDNPP accident is to reproduce the major contaminated area spread northwest from the FDNPP. In order to adequately apply the simulation model, one of the important parameters is source terms (total atmospheric release and temporal change of their release rate) of the FDNPP-derived radionuclides. The source term has been initially evaluated by reverse method (Chino et al., 2011; UNSCEAR, 2013) using monitoring data. Katata et al. (2012) and Terada et al. (2012) updated the temporal emission variations of the radioactive releases. Furthermore, Katata et al. (2015) provided the latest update of the reverse and inverse estimation results after adding an oceanic dispersion model, and further refinement. Hirao et al. (2013) estimated the source term using inverse method by coupling their atmospheric dispersion model and air concentrations and daily deposition data in eastern Japan. Schöppner et al. (2012, 2013), Stohl et al. (2012) and Achim et al. (2014) estimated the source terms by an inverse method using global monitoring data. The total atmospheric releases of the dominant volatile FDNPP-derived radionuclides are summarized in Table 1. The smaller total ^{137}Cs atmospheric releases (less than 10 PBq) (Terada et al., 2012; Hirao et al., 2013), which were estimated using the regional model and only land monitoring data, are underestimates because flow of radioactive plume toward the North Pacific Ocean was not taken into account (Katata et al., 2015). On the other hand, Marzo (2014) pointed out that Stohl et al. (2012) source term appears to overestimate observations.

UNSCEAR (2013) used the source term estimated by Terada et al. (2012), in which the total releases of ^{131}I and ^{137}Cs were estimated to be 120 and 8.8 PBq, respectively, at the lower end of the published values as shown in Table 1. More narrow and precise ranges of the source terms are required to improve the numerical modeling because uncertainties of the atmospheric transport, dispersion and deposition models, especially deposition processes, traded off against uncertainties of the source term (Marzo, 2014). Other uncertainties of the source term resulted from the total inventory of the FDNPP-derived radionuclides in the North Pacific Ocean (Katata et al., 2015). A better estimate of the FDNPP-derived ^{137}Cs inventory in the North Pacific would provide an important constraint of its source term (Inomata et al., 2016).

Modeling studies using meteorological data including

Table 1
Total atmospheric releases of Chernobyl and Fukushima nuclear power plant accidents.

Radionuclide	$T_{1/2}$	Activity (PBq)			
		Chernobyl	Reference	Fukushima	Reference (atmospheric releases)
Noble gases					
^{85}Kr	10.75 y	33	Dreicer et al., 1996	44	Ahlswede et al., 2013
^{133}Xe	5.25 d	6500	Dreicer et al., 1996	15 000	Stohl et al., 2012
				13 400–20 000	Schöppner et al., 2013
				11 400	Eslinger et al., 2014
Volatile elements					
^{129}I	1.57 × 107y	(4–4.8) × 10^{-5}	Aldahan et al., 2007	5.5 × 10^{-5}	Hou et al., 2013
			Kashparov et al., 2003	6.6 × 10^{-5}	Steinhauser et al., 2015
^{131}I	8.03 d	~1760	UNSCEAR, 2008	150	Chino et al., 2011
		1200–1700	Dreicer et al., 1996	130–160	Hamada and Ogino, 2012
				190–380	Winiarek et al., 2012
				65.2	Ten Hoeve and Jacobson, 2012
				150	Hirao et al., 2013
				151	Katata et al., 2015
				124	Tateda et al., 2015
				105.9	Saunier et al., 2013
				200	Kobayashi et al., 2013
				100–200	Akahane et al., 2012
^{134}Cs	2.07 y	~47	Dreicer et al., 1996	11.8	Steinhauser et al., 2015
			UNSCEAR, 2008	18	Hamada and Ogino, 2012
^{137}Cs	30.1 y	85	UNSCEAR, 2008	12	Chino et al., 2011; Winiarek et al., 2012
		74–85	Dreicer et al., 1996	13	Kobayashi et al., 2013
		98	Anspaugh et al., 1988	17	Ten Hoeve and Jacobsen, 2012
				6.1–15	Hamada and Ogino, 2012
				14.5	Katata et al., 2015
				8.8	Terada et al., 2012
				9.6	Hirao et al., 2013
				15.5	Saunier et al., 2013
				10	Achim et al., 2014
				19.3	Winiarek et al., 2014
				35.9	Stohl et al., 2012
				22	Lou Brandon, 2012
				10–20	Akahane et al., 2012

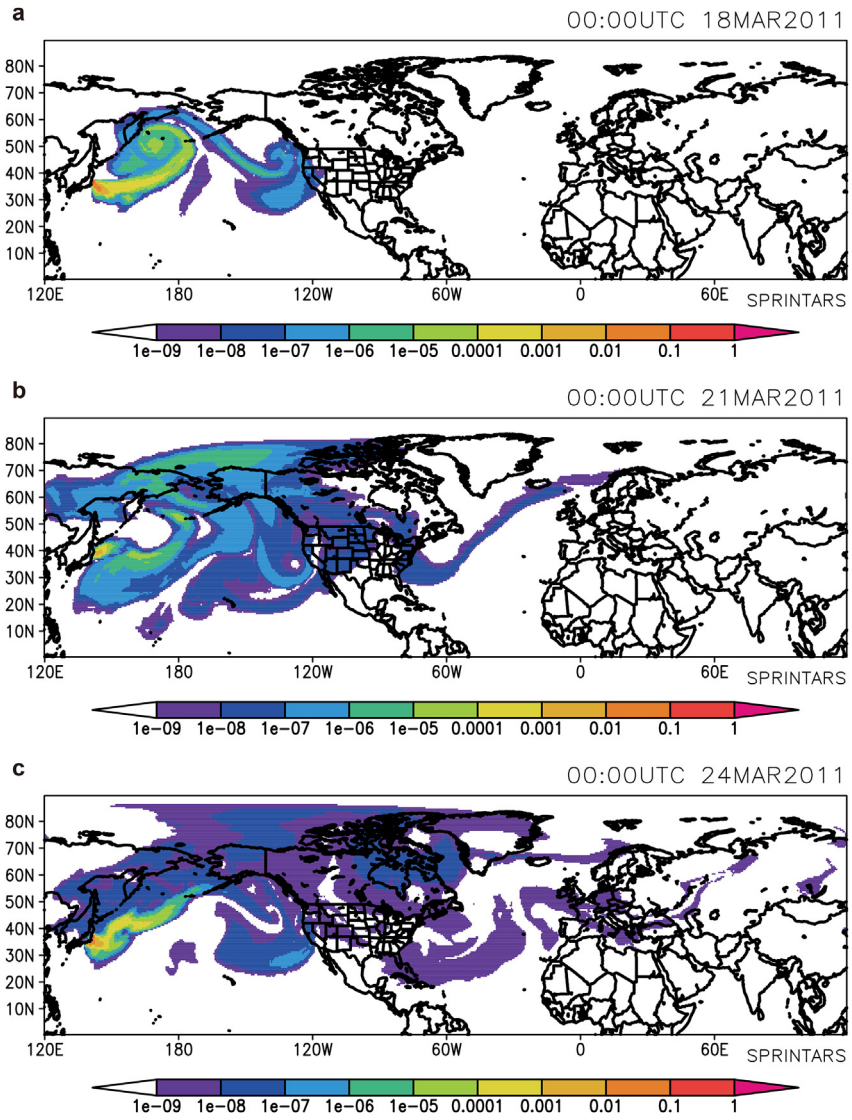

Fig. 5. SPRINTARS simulation of the dispersion of the radioactive cloud for (a) March 18, (b) March 21 and (c) March 24, 2011. This figure used arbitrary unit because constant release rate was assumed for model calculation. Referred from Takemura et al., 2011.

atmospheric processes such as dry and wet depositions and others have already been conducted, from the local scale examining the major contamination episode of March 15th (Chino et al., 2011; Korsakissok et al., 2013), to a more regional scale simulation covering Japan (Morino et al., 2011; Yasunari et al., 2011; Katata et al., 2012; Le Petit et al., 2014; Srinivas et al., 2012; Terada et al., 2012; Draxler et al., 2015; Saito et al., 2015a), and to the global scale (Takemura et al., 2011; Stohl et al., 2012; Sugiyama et al., 2012; Christoudias and Lelieveld, 2013; Povinec et al., 2013c; Marzo, 2014). The local and regional modeling results generally support the case that the high-deposition area over the middle of the Fukushima prefecture was primarily caused by the deposition that occurred on March 15th, which was primarily formed by wet scavenging governed by the land topography of the west of the Fukushima Prefecture (Morino et al., 2011; Draxler et al., 2015; Saito et al., 2015a). The global model, whose typical results are shown in Fig. 5, revealed that about 80% of the total atmospheric release of the FDNPP-derived ^{137}Cs deposited into the North Pacific Ocean (Morino et al., 2011; Ten Hoeven and Jacobson, 2012; Christoudias and Lelieveld, 2013). The World Meteorological Organization (WMO) organized an effort to support the United Nations Scientific Committee on the Effects of Atomic Radiation (UNSCEAR) in its assessment of the FDNPP accident. In this study, deposition and surface air concentrations of the FDNPP-derived radionuclides, in which five different atmospheric transport, dispersion and deposition models (ATDMs) (MLDP0, HYSPLIT, NAME, RATH and FLEXPART) (Draxler et al., 2015) were employed, were simulated to reproduce regional ^{137}Cs deposition observations and ^{131}I and ^{137}Cs air concentration time series at one location about 110 km from the FDNPP. Although the ATDMs were configured identically as much as possible regarding the release duration, release height, concentration grid size and averaging time (Chino et al., 2011; Katada et al., 2012), each ATDM retained its unique treatment of vertical velocity field and the wet and dry deposition. The simulation results revealed that even when using the same meteorological analysis, the each ATDM can produce quite different deposition patterns and that the best model for deposition was not always the best model for air concentrations. Although a single atmospheric transport, dispersion and deposition model (ATDM) could be identified for either deposition or air concentration calculations, overall, the ensemble mean provided more consistent results for both types of calculations. A sensitivity analysis (Marzo, 2014) revealed that the

parameters having the most impact on the results worldwide are the source term and the wet and dry deposition processes, while particle size has very little impact on the model simulation results. Although the atmospheric dispersion models have been improved during the past five years, the variability between observations (deposition) and model simulation is almost within a factor of 10 (Korsakissok et al., 2013; Katata et al., 2015).

3. Oceanic impact of FDNPP-derived radionuclides

3.1. Radioactivity monitoring of ocean

The FDNPP accident caused severe radioactivity contamination of the ocean (Buesseler et al., 2011; Povinec et al., 2013a). Since March 21, 2011, TEPCO measured activity concentrations of gamma-emitting radionuclides in seawater and bottom sediment samples collected in the coastal area within 20 km from the Fukushima Daiichi and Daini NPPs. Markedly high ^{131}I, ^{134}Cs and ^{137}Cs concentrations, which were 5, 1.5 and 1.5 MBq m^{-3}, respectively, were observed in coastal water near outlet of the FDNPP. On March 23, MEXT started marine radioactivity monitoring, in which activity concentrations of gamma-emitting radionuclides in seawater, bottom sediments and dust samples collected on ship-board were determined. Seawater and sediment samples were collected near the coast of the Fukushima and Ibaraki Prefectures and in the sea area 30 km off the coast using the research vessel of the Japan Agency for Marine-Earth Science and Technology (JAMSTEC). Concentrations of ^{131}I and ^{137}Cs in surface seawater were in the ranges from 24.9 to 76.8 kBq m^{-3} and from 11.2 to 24.1 kBq m^{-3}, respectively. After leakage of stagnant water in the accident reactors in early April, Japanese Government announced to expand the monitoring sea area and sampling points on April 5. According to “the plan to step up environmental monitoring” constructed by the Japanese Government on April 25, Japanese Government showed enlarged sea area of radioactivity monitoring on April 25. For the emergency environmental monitoring as the first stage, ^{137}Cs activities in seawater were directly measured by gamma-spectrometry. At the first stage during the period from March to September 2011, a detection limit for sites adjacent the FDNPP was set at 10 kBq m^{-3}. Since October 2011, the detection limit was lowered to 1 kBq m^{-3}, and radioactivity measurements started at south coastal stations in October 2011. At the second stage since

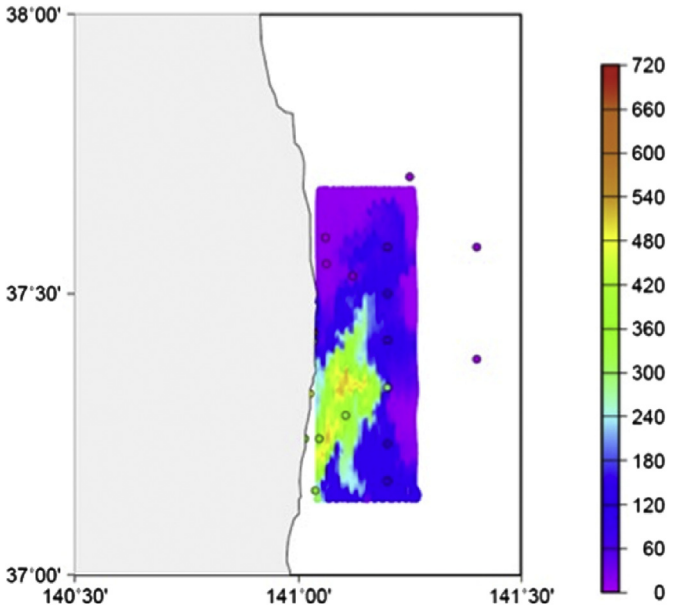

Fig. 7. Spatial distribution of ^{137}Cs concentrations in surface water. (unit: kBq m^{-3}) Referred from Inomata et al., 2014.

April 2012, measurements with a lower detection limit of 2 Bq m^{-3} have been carried out (Hirose, 2015b). The temporal variation of the ^{137}Cs and ^{90}Sr concentrations in coastal water near the FDNPP is shown in Fig. 6. For the coastal area just outside of a 30 km radius from the FDNPP, Oikawa et al. (2013) reported ^{131}I, ^{134}Cs and ^{137}Cs concentrations in surface water during the period from March 23, 2011 to May 7, 2011; the first peak ^{137}Cs in surface water (26 MBq m^{-3}) occurred on March 24, 2011, and after decrease of the surface ^{137}Cs, maximum ^{137}Cs concentration (68 MBq m^{-3}) was observed on April 11, 2011, which corresponded to impacts of atmospheric deposition and direct release of the stagnant water. The spatial distributions of high ^{131}I, ^{134}Cs and ^{137}Cs concentration area were depicted from an aerial radiological survey performed by the U.S. Department of Energy National Nuclear Security Administration on April 18, 2011, in which high radionuclide water spread from south of the FDNPP to northeast offshore area as shown in

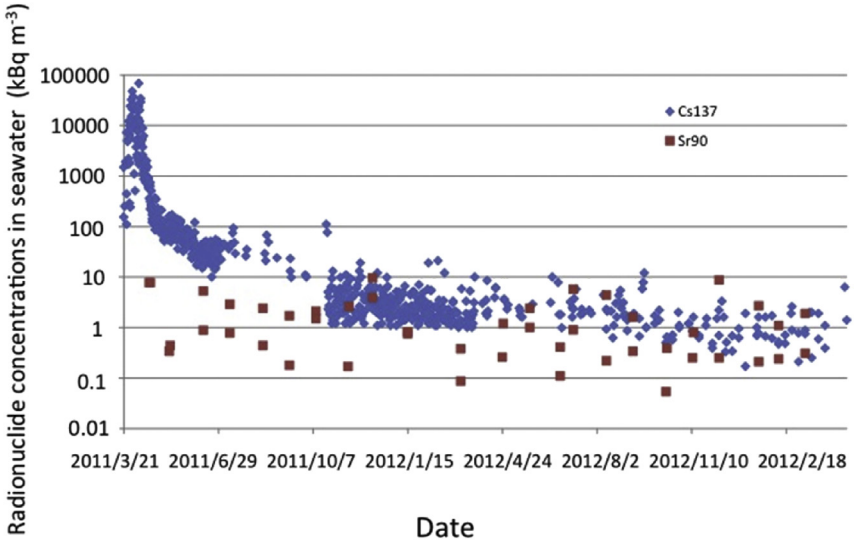

Fig. 6. Temporal variations of ^{137}Cs and ^{90}Sr concentrations in surface water near outlets of the FDNPP. This figure is modified a figure referred from Tsumune et al., (2013).

Fig. 7 (Inomata et al., 2014).

In the late March and early April 2011, extremely high concentrations of ^{131}I, ^{134}Cs and ^{137}Cs in seawater, reached to about 100 MBq m^{-3}, were observed near the FDNPP. As seen in Fig. 6, levels of the FDNPP-derived radionuclides in surface waters rapidly decreased to about 100 kBq m^{-3} until the end of April 2011 (Buesseler et al., 2011; Tsumune et al., 2012). Although the decrease rate of the ^{137}Cs concentrations in seawater declined since May, 2011, higher ^{137}Cs concentrations in seawater, being more than 1 kBq m^{-3}, occurred at stations in the coastal zone until the end of 2015 (Hirose, 2015b; Povinec and Hirose, 2015). Continuous release of the contaminated water was considered as a source controlling higher ^{137}Cs levels in coastal waters (Kanda, 2013; Tsumune et al., 2013).

The FDNPP-derived radionuclides in coastal waters of south and north regions from the FDNPP were determined (Aoyama et al., 2013; Aoyama et al., 2015; Inoue et al., 2012a). For a coastal site at Hasaki, 180 km south of the FDNPP, the ^{137}Cs concentrations in surface water reached a maximum (2.3 kBq m^{-3}) on June 13, 2011, 2 months after the corresponding maximum activity occurred in surface water near outlet of the FDNPP on April 6, 2011, and after that decreased exponentially until September 2011 (Aoyama et al., 2012b). Radiocesium derived from direct release was dominantly transported southward along the coast of the eastern Honshu Island in this period (Aoyama et al., 2012b). For the northeastern Japan Pacific coast about 400 km north of the FDNPP, the FDNPP-derived radiocesium (1.1–2.8 Bq m^{-3} for ^{134}Cs, 2.6–3.9 Bq m^{-3} for ^{137}Cs) was detected in coastal waters in May, 2011 and their peak (37.4 Bq m^{-3} for ^{134}Cs, 42.2 Bq m^{-3} for ^{137}Cs) occurred in August 2011, and after that, it decreased near background values in March 2012 (Kofuji and Inoue, 2013).

Radiocesium released from the FDNPP accident spread in the western North Pacific via two major pathways, i.e. direct discharge of stagnant water from the FDNPP accident site and atmospheric deposition. During April–May 2011, the ^{137}Cs and ^{134}Cs activity concentrations in the North Pacific surface waters ranged from a few Bq m^{-3} to ca. 1 kBq m^{-3}, and from below detection levels (less than 0.4 Bq m^{-3}) to ca. 1 kBq m^{-3} (Aoyama et al., 2012a, 2013; Buesseler et al., 2011, 2012; Honda et al., 2012; Kaeriyama et al., 2013, 2014; Kameník et al., 2013; Oikawa et al., 2013; Ramzaev et al., 2014; Yu et al., 2015). In the northern sea areas of Japan (around Hokkaido) including Japan Sea and in the western sea areas of Japan and around Korea, the ^{134}Cs and ^{137}Cs concentrations in surface water, being less than 3 Bq m^{-3} and less than 1.5 Bq m^{-3}, respectively, were generally low near the background values during the period of June to October, 2011(Inoue et al., 2012a, 2012b, 2012c; Kim et al., 2012).

A high ^{134}Cs and ^{137}Cs concentration (>10 Bq m^{-3}) area, which appeared off the FDNPP of the western North Pacific Ocean due to atmospheric deposition and direct discharge of contaminated water, moved eastward along 40°N latitude following the North Pacific current system including the Kuroshio extension and reached to 165°E during July–September 2011, and to 172°E during October–December 2011. During January–March 2012, the FDNPP-derived radiocesium arrived at the 180° meridian (Aoyama et al., 2012b, 2013). Yoshida et al. (2015) revealed that the easternmost edge of FDNPP-derived ^{134}Cs observed at 174.3°W in 2012 had progressed eastward across the basin to 160.6°W by 2013. In December 2013/January 2014, higher ^{137}Cs concentration (>5 Bq m^{-3}) area appeared in surface waters of the eastern North Pacific Ocean (Fig. 8), whereas the ^{137}Cs concentrations in surface waters of the western North Pacific Ocean except the vicinity of the FDNPP decreased less than 5 Bq m^{-3} (Aoyama et al., 2015). Smith et al. (2015) revealed that the FDNPP-derived radiocesium had been transported off the west coast of Canada by August 2014.

Chemical tracer studies revealed transport processes of anthropogenic radionuclides into ocean interior of the North Pacific Ocean, which is called “subduction”; nuclear bomb-derived ^{137}Cs showed two maxima at a potential density of 25.5 and at a potential density of 26.0, corresponding to the subtropical mode water (STMW) and the central mode water (CMW), respectively (Aoyama et al., 2008). Most of the FDNPP-derived ^{134}Cs and ^{137}Cs existed in surface layer during the period of April – May 2011 (Honda et al., 2012; Aoyama et al., 2015). In December 2011–February 2012, the ^{134}Cs and ^{137}Cs peaks corresponding to the STMW and the CMW appeared in their vertical profiles in the western North Pacific Ocean (Kumamoto et al., 2013). Cross sections of ^{134}Cs and ^{137}Cs activities along 165°E observed in June/July 2012 (Fig. 9) revealed

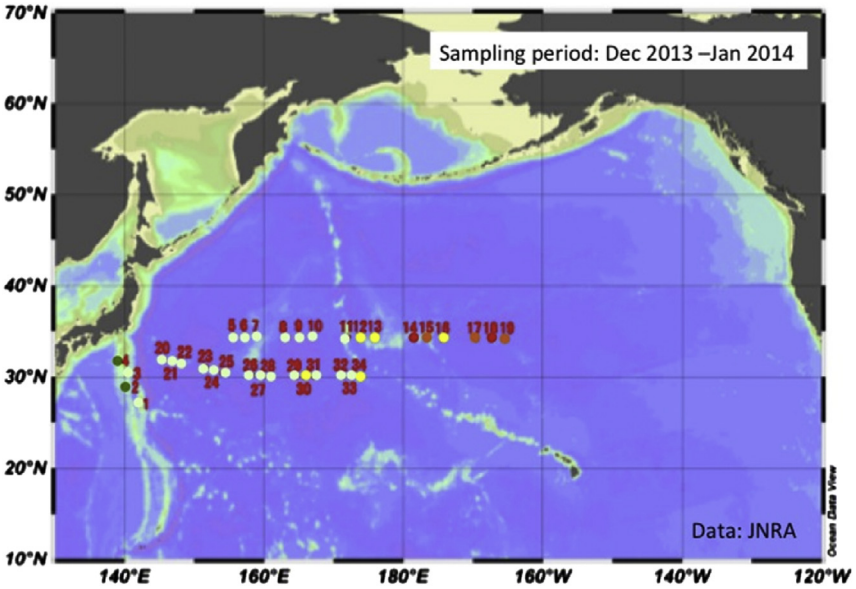

Fig. 8. Spatial distribution of ^{137}Cs concentrations in surface water during the period from December 2013 to January 2014. This figure is depicted from data cited from JNRA homepage. Green circle: <2 Bq m^{-3}, pale green circle: 2–3 Bq m^{-3}, yellow circle: 3–4 Bq m^{-3}, orange circle: 4–5 Bq m^{-3}, red circle: >5 Bq m^{-3}. (For interpretation of the references to color in this figure legend, the reader is referred to the web version of this article.)

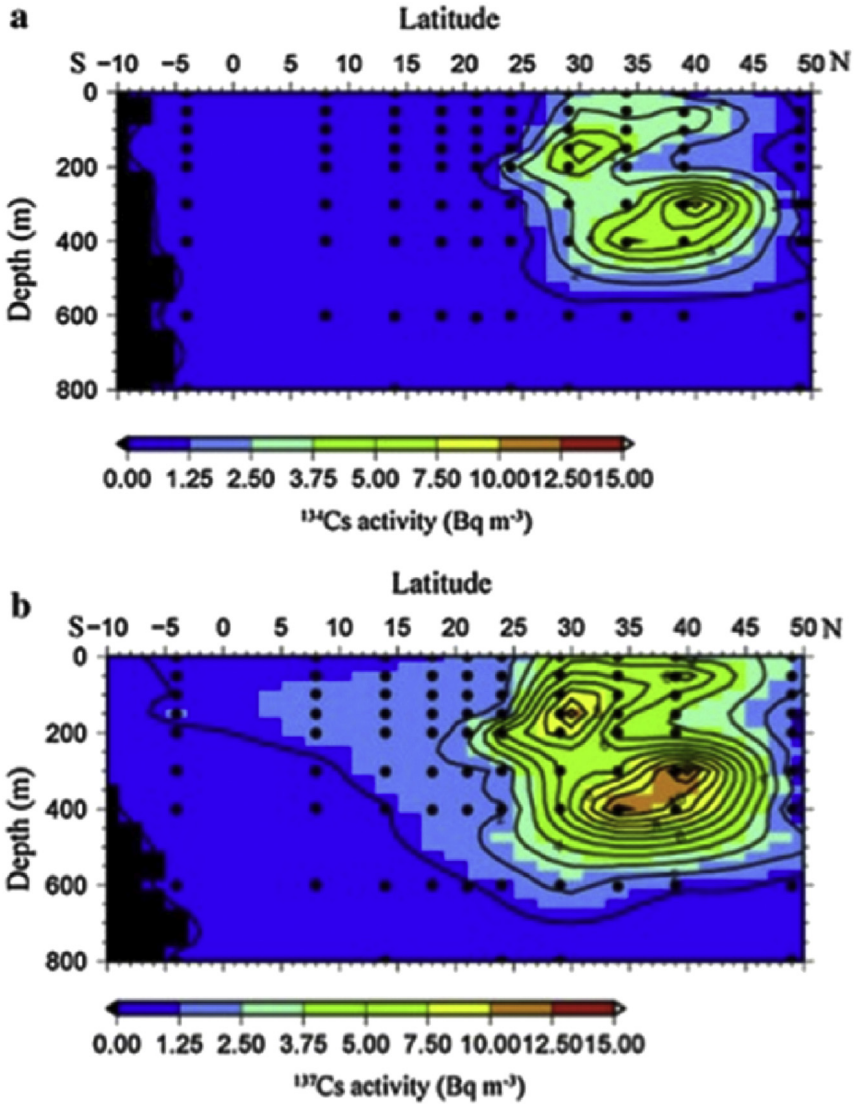

Fig. 9. Transects of ^{134}Cs and ^{137}Cs concentrations in seawater along 165°E. Referred from Aoyama et al., 2015.

that two maxima occurred at a potential density range (25.1–25.3) in latitude range (24°N–29°N) and at a potential density range (26.1–26.3) in latitude range (34°N–39°N), corresponding to the STMW and CMW, respectively (Aoyama et al., 2015). The similar subsurface maxima of the FDNPP-derived ^{134}Cs and ^{137}Cs were observed in the western North Pacific (Kaeriyama et al., 2013; Kumamoto et al., 2014; Men et al., 2014; Yoshida et al., 2015). These subsurface maxima are formed by subduction accompanied with production of the STMW and CMW and transported southwestward according to the North Pacific Subtropical gyre (Aoyama et al., 2011; Kaeriyama et al., 2014; Kumamoto et al., 2014; Yoshida et al., 2015). Meso-scale eddies play an important role of transport and dispersion of the FDNPP-derived radionuclides in the western North Pacific (Buesseler et al., 2012; Masumoto et al., 2012). The highest concentrations of ^{134}Cs and ^{137}Cs in seawater collected in June and July 2012 were observed inside the meso-scale anticyclonic eddies (Budyansky et al., 2015). The maximum radiocesium concentrations occurred not at the surface but within subsurface and intermediate water layers (100–500 m), which corresponded to the potential density range of 26.5–26.7 inside the low potential vorticity cores of the eddies.

Particle scavenging is considered as a candidate of vertical transport of anthropogenic radionuclides. Although most of the radiocesium exist in a dissolved form, a part of the FDNPP-derived radiocesium was included in suspended matter (Honda and Kawakami, 2014). Honda et al. (2013, Honda and Kawakami, 2014) revealed that particulate radiocesium was rapidly transported in deep layer by employment of time series sediment traps; the FDNPP-derived ^{137}Cs was first detected at 500 m depth (4810 m) about two weeks (one month) after the FDNPP accident.

After the FDNPP accident, ^{89}Sr, ^{90}Sr, ^{129}I and ^{3}H, which exhibit minor impacts to environment, were measured in seawater (Casacuberta et al., 2013; Povinec et al., 2012a, 2013b). At the site 15 km off the FDNPP, the high ^{89}Sr (69 kBq m^{-3}) and ^{90}Sr (9.3 kBq m^{-3}) concentrations in surface water were observed on 18 April 2011, in which the observed ^{90}Sr levels are about four orders of magnitude greater than the pre-Fukushima level (1.2 Bq m^{-3}) (Povinec et al., 2012a). Sporadic high ^{90}Sr in coastal water near the FDNPP (400 kBq m^{-3}) occurred after accidental leakage of treated water on December 4, 2011. For offshore Fukushima approximately from 30 km to 600 km from the coast, the ^{129}I and ^{3}H levels in surface waters in June 2011 varied between 0.01 and 0.8 mBq m^{-3}, and 0.05–0.15 kBq m^{-3}, respectively, which were higher than the global fallout level by factors of about 50 and 3, respectively

(Povinec et al., 2013b). Concentrations of ^{90}Sr and ^{89}Sr in surface waters and shallow profiles ranged from 0.8 to 85 Bq m^{-3} and from 19 to 265 Bq m^{-3}, respectively (Casacuberta et al., 2013). As did ^{137}Cs, ongoing release of ^{90}Sr (2.3–8.5 GBq d^{-1}) occurred in the coastal water near the FDNPP in September 2013 (Castrillejo et al., 2015), as seen in Fig. 6. On the other hand, there is no evidence of presence of FDNPP-derived plutonium in seawater using plutonium isotope signatures (Bu et al., 2014).

3.2. Ocean dispersion model of radionuclides and estimation of total budgets

Numerical simulation on oceanic dispersion of nuclear bomb-derived ^{137}Cs using global circulation model has been developed during the past two decades (Tsumune et al., 2003; Nakano et al., 2010). Oceanic numerical simulation is useful for estimating the direct release rate of radionuclides derived from contaminated water and for presenting and predicting oceanic dispersion of radioactive materials. Significant amounts of radionuclides emitting into atmosphere following the FDNPP accident fell down in ocean surface. In order to have increasing reliability of the model simulation, one of the most important parameters is source term. The total amount of ^{137}Cs or ^{134}Cs injected into the North Pacific via the atmospheric deposition was estimated to be around 6 PBq by previous studies (Morino et al., 2011; Stohl et al., 2012) out of 9 PBq, which was the total amount of ^{137}Cs or ^{134}Cs released to the atmosphere (Terada et al., 2012). In addition, highly contaminated stagnant water was directly discharged into ocean. To assess environmental effects of the FDNPP-derived radionuclides, it is important to evaluate total amounts of the FDNPP-derived radionuclides due to the direct release. Tsumune et al. (2012) estimated direct release rates of ^{131}I, ^{134}Cs and ^{137}Cs by an inverse method using a regional ocean model simulation and observation data, in which a started time of the direct release was evaluated on March 26, 2011 from ^{131}I/^{137}Cs activity ratios. The total amount of ^{137}Cs derived from the direct release was estimated 3.5 ± 0.7 PBq. On the other hand, Bailly du Bois et al. (2012) reported higher estimate of the total direct-release ^{137}Cs from observation data. As a result, estimates of total amount of ^{137}Cs or ^{134}Cs discharged directly to the ocean ranged widely from 3.5 PBq to 27 PBq (Estournel et al., 2012; Tsumune et al., 2012, 2013; Bailly du Bois et al., 2012; Miyazawa et al., 2013; Rypina et al., 2013). On the other hand, the inventory of the FDNPP-derived ^{134}Cs in the North Pacific Ocean was estimated to be 15.3 ± 2.6 PBq applying an optimal interpolation technique to the oceanic distribution of ^{134}Cs (Inomata et al., 2016). After direct discharge of huge amounts of the FDNPP-derived radionuclides during the period of March–April, 2011, smaller amounts of radiocesium were continuously released into ocean from the FDNPP; average release rates of ^{137}Cs in summer 2011 and summer 2012 was estimated to be 93 and 8.1 GBq d^{-1}, respectively, taken into account a quasi-steady state model of continuous water exchange between the harbor and open ocean (Kanda, 2013).

Modeling studies using oceanographic data including oceanic processes such as diffusion, advection and others have already been conducted from a local/regional scale simulation covering off Fukushima (Kawamura et al., 2011; Dietze and Kriest, 2012; Masumoto et al., 2012; Miyazawa et al., 2012; Tsumune et al., 2012; Estournel et al., 2012; Masumoto et al., 2012; Choi et al., 2013; Min et al., 2013; Periáñez et al., 2012, 2015) to the basin scale (Nakano and Povinec., 2012; Behrens et al., 2012; Tsumune et al., 2013; Rossi et al., 2013, 2014; Kawamura et al., 2014). The local and regional modeling results generally support the case that the high-concentration area along the Fukushima coast was primarily caused by coastal current prevailing south–north current along cost line (Tsumune et al., 2013) and eddy-like structure, which contributed to dispersion of ^{137}Cs in areas beyond continental shelf (Masumoto et al., 2012). Some comparison exercises regarding model performances when applied to simulate the releases from the FDNPP have been carried out (Masumoto et al., 2012; Periáñez et al., 2015). The exercise results presented a significant variability (several orders of magnitude) between model outputs, even in a point very close to Fukushima outlet (Periáñez et al., 2015). This variability in model results can be primarily attributed to the different descriptions of hydrodynamics in each model.

According to the basin-scale model, the dispersion of the FDNPP-derived ^{137}Cs deposited into the North Pacific Ocean was forecasted for a few decades after the FDNPP accident, taken into account the atmospheric deposition and the direct release (Nakano and Povinec, 2012). Typical results of the numerical simulation are shown in Fig. 10. Main FDNPP-derived radiocesium released to coastal waters would reach the coast of North America after 5–6 years and ^{137}Cs concentrations would be nearly homogeneous over the whole Pacific after 10 years (Behrens et al., 2012). The ^{137}Cs concentrations in the surface, intermediate, and deep layers reduce to the pre-Fukushima levels over the North Pacific some 2.5 years after the FDNPP accident, in which the meso-scale eddies in the Kuroshio Extension played an important role in diluting the ^{137}Cs patch (Kawamura et al., 2014). Rossi et al. (2013, 2014) also suggested that the Fukushima plume is rapidly diluted within the Kuroshio system over a time-scale of a few months and that a component of Fukushima ^{137}Cs will be injected into the interior ocean via subduction.

4. Socioeconomic impact

The FDNPP accident caused huge socioeconomic impacts to Japan. About 150 000 people have been evacuated from the contaminated zone, mainly within a radius of 20 km from the FDNPP. Evacuation of hospitals faced difficulties and it has been estimated that some 60 patients died from complications related to the evacuation. Although some limited return has started, most of the residents in the major contaminated areas still face difficulties in returning at the end of 2015. These impacts are partly resulting from the radiological effects due to occurrence of highly radioactivity-contaminated areas and problems related to food safety. UNSCEAR report (2013) mentioned that a general-related increase in the incidence of health effects among the exposed population would not be expected to be discernible over the baseline. Evangeliou et al. (2014) evaluated global and local cancer risks after the FDNPP accident using the atmospheric transport model. Although the higher source term of Stohl et al. (2012) and the LNT assumption were adopted for the risk evaluation, the FDNPP accident in Japan presents a negligible radiological risk, both in terms of cancer incidents and deaths, with a peak in the adjacent regions of the FDNPP much lower in comparison to the Chernobyl accident, which were due to the lower emissions and also because most of the radiocesium released from the FDNPP was deposited in the North Pacific Ocean. However, evacuation of residents accompanied with the FDNPP accident destroyed local communities; in 2015, significant amounts of residents are still evacuated from restricted and deliberated evacuation areas near the FDNPP site. Long-term psychological effects including depression, anxiety, fear and unexplained physical symptoms, which have been found to increase after the Chernobyl accident (Bromet, 2012), occurred after the FDNPP accident as well.

For remediation of environment, the Government has planned to cleanup of contaminated areas having external radiation doses above 5 mSv y^{-1}, in order to reduce exposure and allow displaced residents to return home (Hardie and McKinley, 2014). Established, modified and newly developed techniques for regional remediation

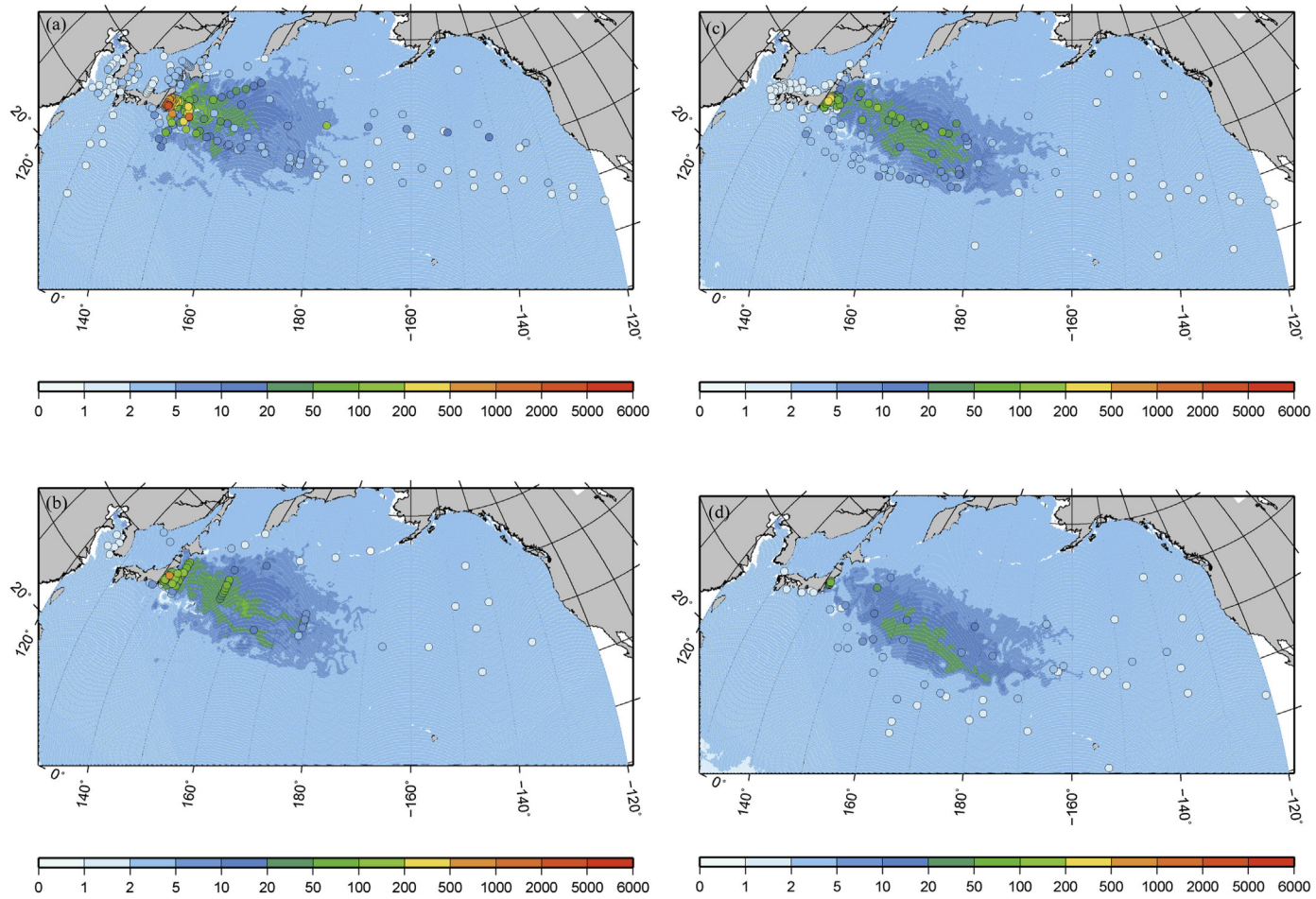

Fig. 10. Spatial distributions of ^{137}Cs concentrations (Bq m^{-3}) in surface water. (a) on 15 May 2011 and measurements from April to June 2011; (b) Simulated ^{137}Cs concentrations (Bq m^{-3}) on 15 August 2011 and observed values (circle) from July to September 2011; (c) on 15 November 2011 and observed values from October to December 2011; (d) on 15 February 2012 and observed values from January to March 2012. Referred from Tsumune et al., 2013.

have been tested under the realistic field and their performance characteristics determined. As a result, the FDNPP accident resulted in economic loss of billions of dollars due to cleanup costs and reduced economic activity in areas affected by radioactivity (Brumfiel and Fuyuno, 2012). On the other hand, huge amounts of radioactive wastes have been put in temporary storage, although most of the contaminated forest areas have not been cleaned up as of 2015. The output from these activities related to environment remediation must, however, be considered "living documents" that will evolve as more experience is gained during further cleanup work.

Radiological contamination of agricultural foodstuffs and drinking water was concerned after large atmospheric emissions of the FDNPP-derived radionuclides. Hamada and Ogino (2012) documented the response of the Japan Government to food safety regulations after the nuclear accident. According to notification of the provisional "Guideline values for food and drink intake restrictions", any foodstuffs and drinking water containing radionuclides exceeding regulation values were prohibited to consume. The radionuclide monitoring revealed that their levels in foodstuffs (vegetables and raw milk) in Kanto area and Fukushima exceeded the provisional regulation values in late March 2011. Therefore the Government provided instructions to restrict consumption of food, agricultural products and drinking water to relevant governors of the prefectures. On April 2012, the Government lowered the provisional regulation value of radiocesium for internal exposure from food intake; the new value for the protective actions of food intake was 100 Bq kg^{-1} w.w. (wet weight) for radiocesium (Povinec et al., 2013a). The change of the provisional regulation values would enhance psychological influences of intakes of foodstuffs containing radioactivity. In 2012, the levels of the FDNPP-derived radionuclides in agricultural products were lower than the provisional regulation values. For marine products, however, higher radiocesium concentrations that exceeded the regulation value were found in fishes caught in shallow waters near the FDNPP, although the radiocesium concentrations in fishes, which showed large variability among taxa, habitats and others, decreased (Buesseler, 2012; Wada et al., 2013; Povinec and Hirose, 2015). Tateda et al. (2015) studied biokinetics of ^{137}Cs in olive flounder using a dynamic biological compartment model, in which the maximum radiocesium concentrations in fish throughout the plankton food chain is likely to be the initial radiocesium concentration which they were exposed during the contamination stage. Povinec and Hirose (2015) evaluated the total effective dose commitment from ingestion of radionuclides in fish, shellfish and seaweed caught in coastal waters off Fukushima, which was calculated to be 0.6 ± 0.4 mSv y^{-1}, whereas for consumption of fish caught in the open Pacific Ocean, it was estimated to be 0.07 ± 0.05 mSv y^{-1}. The estimated individual doses have been below the levels where any health damage of the Japanese and world population could be

expected. Irrespective of low radiological risk on consumption of marine product, the restriction of the consumption of fishes caught in the coastal area near the FDNPP has continued. There is socio-economic impact of the FDNPP related to consumption of fishes, including export problems of marine products. However, it should be also mentioned that local fishery industry has been heavily damaged mainly due to the direct effects of the devastating tsunami.

Another socioeconomic impact was derived from the electricity supply. Before the FDNPP accident, 54 nuclear reactors supplied about 30% of the electricity in Japan. A number of reactors shut down automatically due to the earthquake. Others were successively shut down as power reactors started their annual refueling maintenance outage. By the beginning of May 2012 all Japanese power reactors were shut down. Although restart of more reactors took time, partly due to the need for technical safety improvements, partly due to loss of trust in the nuclear industry and government authorities, and delaying local political approval, in August 2015, a nuclear power reactor restarted after new safety review and local government approval. The loss of nuclear electricity production has been partially offset by stepping up production from fossil-fueled plants but a number of electricity-saving measures have also been necessary. Imports of fossil fuels have been increased to the extent significantly affecting the Japanese trade balance, and CO_2 emissions have increased. The total cost of the FDNPP accident in a 50-year perspective are difficult to predict, but different cost estimates lie presently in the range of 100–500 billion US$, corresponding to about 2–10% of Japan's annual gross domestic product (Högberg, 2013).

5. Conclusion

The FDNPP accident severely affected the environment, although the environmental and radiological consequences caused by the Chernobyl nuclear accident in 1986 exceeded those of the FDNPP accident in almost every respect. However, the highly radioactivity-contaminated area was restricted to the Japanese territory including EEZ of Ocean. Japanese researchers and experts have contributed to the radioactivity monitoring including mapping of the deposited FDNPP-derived radionuclides. The FDNPP-derived radionuclides in surface air and deposition were detected by monitoring networks in the world including CTBTO and monitoring sites in individual countries in the northern Hemisphere. For marine radioactivity monitoring, international expeditions have been conducted in the North Pacific. Short and long-term variability of the FDNPP-derived radionuclides in air and deposition, which primarily reflected dispersion of the radioactive plume, have been recorded. The contamination map and its time revolution for the deposition densities on land and radionuclide concentrations in seawater were observed; land and ocean surveys played important roles to depict high radioactivity-contaminated area. These monitoring data were used not only to ensure radiation protective actions for residents but also to elucidate consequence of the FDNPP accident. In another point of view, the FDNPP accident has given an opportunity to have better understanding of the atmospheric and oceanic dispersion processes.

For the FDNPP accident, numerical model simulations, including local, regional and global scale modeling, were applied to atmosphere and ocean; the first purpose is to know source terms, second one is to reproduce atmospheric and oceanic dispersions of the FDNPP-derived radionuclides, and third one is to predict their dispersion and fate. Especially local and regional-scale models are expected to predict dispersion of the radioactive cloud and to elucidate highly contaminated areas to support the protective action planning. The numerical models were applied to estimate the source terms comprising time-sequence of atmospheric emission rates and total release amount of the FDNPP-derived radionuclides. Recent development of the atmospheric transport, dispersion and deposition model allows us to reproduce the pathway of the radioactive cloud and high radioactive deposition area, although large uncertainties are still present. The global-scale model simulations were employed to elucidate worldwide dispersion of the FDNPP-derived radionuclides, whose results are useful to compare CTBTO experimental data with modeling results. Atmospheric modeling, ocean circulation models, including regional and basin-scale modeling, were employed to estimate the source terms including direct release of the radioactivity-contaminated stagnant water and atmospheric deposition and to predict transport and dispersion of radioactive patches in the North Pacific Ocean at several years to decadal time scale. The monitoring data for the FDNPP accident, which would be compiled as a database, will be useful for verification of numerical model simulations and improvement of numerical modeling.

The results of the FDNPP accident show that severe nuclear reactor accidents are not unique in terms of the number of directly attributable fatalities resulting from accidents related to energy production such as dam collapses. USNRC (2012) has estimated that with proper off-site emergency response programs, the contribution to individual fatality risk (early and late radiation-induced fatalities) from severe reactor accidents is small to other individual health risks, even with release of ^{137}Cs in the ranges of several PBq. Until now, assessments of the radiological health consequences of the Fukushima accident do not seem to contradict these estimates. However, severe NPP accidents with radioactive releases in the range of several PBq may cause environmental and socio-economic consequences due to the large-scale and long-lived ground contamination with associated human and monetary costs. Högberg (2013) concluded that the FDNPP accident, as did the Chernobyl and TMI accidents, had the root causes in system deficiencies indicative of poor safety management and poor safety culture in both the nuclear industry and government authorities.

Finally, the levels of the FDNPP-derived radionuclides, especially ^{137}Cs, ^{134}Cs and ^{90}Sr, in the atmosphere and seawater near the FDNPP in 2015 have still been higher than background levels. These results strongly suggest that continuous monitoring of anthropogenic radionuclides in atmospheric and oceanic samples is still required.

Acknowledgments

Author thanks S. Sheppard and S. Hisamatsu, editors of Journal of Environmental Radioactivity, to have an opportunity to write a review paper and for valuable comments and suggestion. Author also acknowledges P.P. Povinec for constructive comments and suggestion.

References

Achim, P., Monfort, M., Le Petit, G., Gross, P., Douysset, G., Taffary, T., Blanchard, X., Moulin, C., 2014. Analysis of radionuclide releases from the Fukushima Dai-ichi nuclear power plant accident Part II. Pure Appl. Geophys. 171, 645–667.

Adachi, K., Kajino, M., Zaizen, Y., Igarashi, Y., 2013. Emission of spherical cesium-bearing particles from an early stage of the Fukushima nuclear accident. Sci. Rep. 3, 2554. http://dx.doi.org/10.1038/srep02554.

Ahlswede, J., Hebel, S., Ross, J.O., Schoetter, R., Kalinowski, M.B., 2013. Updata and improvement of the global krypton-85 emission inventory. J. Environ. Radioact. 115, 34–42.

Akahane, K., Yonai, S., Fukuda, S., Miyahara, N., Yasuda, H., Iwaoka, K., Matsumoto, M., Fukumura, A., Akashi, M., 2012. The Fukushima nuclear power plant accident and exposures in the environment. Environmentalist 32, 136–143.

Aldahan, A., Alfimov, V., Possnert, G., 2007. 129I anthropogenic budget: major sources and sinks. Appl. Geochem. 22, 606–618.

Amano, H., Akiyama, M., Chunlei, B., Kawamura, T., Kishimoto, T., Kuroda, T., Muroi, T., Odaira, T., Ohota, Y., Takeda, K., Watanabe, Y., Morimoto, T., 2012. Radiation measurements in the Chiba Metropolitan area and radiological aspects of fallout from the Fukushima Daiichi Nuclear Power Plants accident. J. Environ. Radioact. 111, 42–52.

Anspaugh, L.R., Catlin, R.J., Goldman, M., 1988. The global impact of the chernobyl reactor accident. Science 242, 1513–1519.

Aoyama, M., Hirose, K., Nemoto, K., Takatsuki, T., Tsumune, D., 2008. Water mass labeled with global fallout ^{137}Cs formed by subduction in the North Pacific. Geophys. Res. Lett. 35, L01604.

Aoyama, M., Fukasawa, M., Hirose, K., Hamajima, M., Kawano, T., Povinec, P.P., Sanchez-Cabeza, J.A., 2011. Cross equator transport of ^{137}Cs from North Pacific Ocean to South Pacific Ocean (BEAGLE2003 cruises). Prog. Oceanogr. 89, 7–16.

Aoyama, M., Hamajima, Y., Hult, M., Uematsu, M., Oka, E., Tsumune, D., Kumamoto, Y., 2015. ^{134}Cs and ^{137}Cs in the North Pacific Ocean derived from the March 2011 TEPCO Fukushima Dai-ichi Nuclear Power Plant accident Japan. Part one: surface pathways and vertical distibutions. J. Oceanogr. http://dx.doi.org/10.1007/s10872-015-0335-z.

Aoyama, M., Tsumune, D., Hamajima, Y., 2012a. Distribution of ^{134}Cs and ^{137}Cs in the North Pacific Ocean: impacts of the TEPCO Fukushima Daiichi NPP accident. J. Radioanal. Nucl. Chem. 296, 535–539.

Aoyama, M., Tsumune, D., Uematsu, M., Kondo, F., Hamajima, Y., 2012b. Temporal variation of ^{134}Cs and ^{137}Cs activities in surface water at stations along the coastline near the Fukushima Dai-ichi Nuclear Power Plant accident site. Jpn. Geochem. J. 46, 321–325.

Aoyama, M., Uematsu, M., Tsumune, D., et al., 2013. Surface pathway of radioactive plume of TEPCO Fukushima NPP1 released ^{134}Cs and ^{137}Cs. Biogeosciences 10, 3067–3978.

Baeza, A., Corbacho, J.A., Rodriguez, A., Galvan, J., Garcia-Tenorio, R., Manjon, G., et al., 2012. Influence of the Fukushima Dai-ichi nuclear accident on Spanish environmental radioactivity levels. J. Environ. Radioact. 114, 138–145.

Bailly du Bois, P., Laguionie, P., Boust, D., Korsakissok, I., Didier, D., Fievet, B., 2012. Estimation of marine source-term following Fukushima Dai-ichi accident. J. Environ. Radioact. 114, 2–9.

Barsanti, M., Conte, F., Delbono, I., Iuriaro, G., Battisti, P., Bortoluzzi, S., et al., 2012. Environmental radioactivity analyses in Italy following the Fukushima Dai-ichi nuclear accident. J. Environ. Radioact. 114, 126–130.

Behrens, E., Schwarzkopf, F.U., Lubbecke, J., Boning, C.W., 2012. Mosel simulations on the long-term dispersal of ^{137}Cs released into the Pacific Ocean off Fukushima. Environ. Res. Lett. 7, 034000.

Beresford, N.A., Barnett, C.L., Howard, B.J., Howard, D.C., Wells, C., Tyler, A.N., et al., 2012. Observations of Fukushima fallout in Great Britain. J. Environ. Radioact. 114, 48–53.

Biegalski, S.R., Bowyer, T.W., Eslinger, P.W., Friese, J.A., Greenwood, L.R., Haas, D.A., Hayes, J.C., Hoffman, I., Keillor, M., Miley, H.S., Moring, M., 2012. Analysis of data from sensitive U.S. monitoring stations for the Fukushima Dai-ichi nuclear reactor accident. J. Environ. Radioact. 114, 15–21. http://dx.doi.org/10.1016/j.jenvrad.2011.11.007.

Bikit, I., Mrda, D., Todorovic, N., Nikolov, J., Krmar, M., Veskovic, M., et al., 2012. Airborne radioiodine in northern Serbia from Fukushima. J. Environ. Radioact. 114, 89–93.

Bowyer, T.W., Biegalski, S.R., Cooper, M., Eslinger, P.W., Haas, D., Hayes, J.C., et al., 2011. Elevated radioxenon detected remotely following the Fukushima nuclear accident. J. Environ. Radioact. 102, 681–687.

Bromet, E.J., 2012. Mental health consequences of the Chernobyl disaster. J. Radiol. Prot. 32, N71–N75.

Brumfiel, G., Fuyuno, I., 2012. Japan's nuclear crisis: Fukushima's legacy of fear. Nature 483, 138–140.

Bu, W., Zheng, J., Guo, Q.J., Aono, T., Tagami, K., Uchida, S., Tazoe, H., Yamada, M., 2014. Ultra-trace plutonium determination in small volume seawater by sector field inductively coupled plasma mass spectrometry with application to Fukushima seawater samples. J. Chromatogr. A 1337, 171–178.

Budyansky, M.V., Goryachov, V.A., Kaplunenko, D.D., Lobanov, V.B., Prants, S.V., Sergeev, A.F., Shlyk, N.V., Uleysky, M.Yu., 2015. Role of mesoscale eddied in transport of Fukushima-derived cesium isotopes in the ocean. Deep-Sea Res. I 96, 15–27.

Buesseler, K.O., 2012. Fishing for answers off Fukushima. Science 338, 480–482.

Buesseler, K.O., Aoyama, M., Fukasawa, M., 2011. Impacts of the Fukushima Nuclear Power Plants on Marine radioactivity. Environ. Sci. Technol. 45, 9931–9935.

Buesseler, K.O., Jayne, S.R., Fisher, N.S., Rypina, I.I., Baumann, H., Baumann, Z., Breier, C.F., Douglass, E.M., George, J., Macdonald, A.M., Miyamoto, H., Nishikawa, J., Pike, S.M., Yoshida, S., 2012. Fukushima-derived radionuclides in the ocean and biota off Japan. Proc. Natl. Acad. Sci. U. S. A. 109, 5984–5988.

Carvalho, F.P., Reis, M.C., Oliveira, J.M., Malta, M., Silva, L., 2012. Radioactivity from Fukushima nuclear accident detected in Lisbon, Portugal. J. Environ. Radioact. 114, 152–156. http://dx.doi.org/10.1016/j.jenvrad.2012.03.005.

Casacuberta, N., Masque, P., Garcia-Orellana, J., Garcia-Tenorio, R., Buesseler, K.O., 2013. ^{90}Sr and ^{89}Sr in seawater off Japan as a consequence of the Fukushima Dai-ichi nuclear accident. Biogeosciences 10, 3649–3659.

Castrillejo, M., Casacuberta, N., Breier, C.F., Pike, S.M., Masquè, P., Buesseler, K.O., 2015. Reassessment of ^{90}Sr, ^{137}Cs, and ^{134}Cs in the coast off Japan derived from the Fukushima Dai-ichi nuclear accident. Environ. Sci. Technol. http://dx.doi.org/10.1021/acs.est.5b03013.

Chino, M., Nakayama, H., Nagai, H., Terada, H., Katata, G., Yamazawa, H., 2011. Preliminary estimation of released amounts of ^{131}I and ^{137}Cs accidentally discharged from the Fukushima Daiichi nuclear power plant into the atmosphere. J. Nucl. Sci. Technol. 48, 1129–1134.

Choi, Y., Kida, S., Takahashi, K., 2013. The impact of oceanic circulation and phase transfer on the dispersion of radionuclides released from the Fukushima Dai-ichi Nuclear Power Plant. Biogeosciences 10, 4911–4925.

Christoudias, T., Lelieveld, J., 2013. Modelling the global atmospheric transport and deposition of radionuclides from the Fukushima Dai-ichi nuclear accident. Atmos. Chem. Phys. 13, 1425–1438.

Clemenza, M., Fiorini, E., Previtali, E., Sala, E., 2012. Measurement of airborne ^{131}I, ^{134}Cs and ^{137}Cs due to the Fukushima reactor incident in Milan (Italy). J. Environ. Radioact. 114, 113–118. http://dx.doi.org/10.1016/j.jenvrad.2011.12.012.

Cosma, C., Iurian, A.R., Nita, D.C., Begy, R., Cindea, C., 2011. Considerations about the presence of Fukushima radionuclides in the NW part of Romania. Rom. J. Physiol. 56, 1199–1207.

CTBTO. http://www.ctbto.org/press-centre/highlights/2011/fukushima-related-measurements-by-the-ctbto/.

De Vismes Ott, A., Gurriaran, R., Cagnat, X., Masson, O., 2013. Fission product activity ratios measured at trace level over France during the Fukushima accident. J. Environ. Radioact. 125, 6–16.

Dietze, H., Kriest, I., 2012. ^{137}Cs off Fuksuhima Dai-ichi, Japan – model based estimates of dilution and fate. Ocean Sci. 8, 319–332.

Doi, T., Masumoto, K., Toyoda, A., Tanaka, A., Shibata, Y., Hirose, K., 2013. Anthropogenic radionuclides in the atmosphere observed at Tsukuba: characteristics of the radionuclides derived from Fukushima. J. Environ. Radioact. 122, 55–62.

Draxler, R., Arnold, D., Chino, M., Galmarini, S., Hort, M., Jones, A., Leadbetter, S., Malo, M., Maurer, S., Rolph, G., Saito, K., Servranckx, R., Shinbori, T., Solazzo, E., Watowa, G., 2015. World meteorological organization's model simulations of the radionuclides dispersion and deposition from the Fukushima Daiichi nuclear power plant accident. J. Environ. Radioact. 139, 172–184.

Dreicer, M., Aakrog, A., Alexakhin, R., Anspaugh, L., Arkhipov, N.P., Johansson, K.-J., 1996. Consequences of the Chernobyl accident for the natural and human environments. In: EC, IAEA, WMO (Eds.), One Decade after Chernobyl: Summing up the Consequences of the Accident, Vienna, pp. 319–361.

Eslinger, P.W., Biegalski, S.R., Bowyer, T.W., Cooper, M.W., Haas, D.A., Hayes, J.C., Hoffman, I., Korpach, E., Miley, H.S., Rishel, J.P., Ungar, K., White, B., Woods, V.T., 2014. Source term estimation of radioxenon released from the Fukushima Dai-ichi nuclear reactors using measured air concentrations and atmospheric transport modeling. J. Environ. Radioact. 127, 127–132.

Estournel, C., Bosc, E., Bocquet, M., Ulses, C., Marsaleix, P., Winiarek, V., Osvath, I., Nguyen, C., Duhaut, T., Lyard, F., Michaud, H., Auclair, F., 2012. Assessment of the amount of cesium-137 released into the Pacific Ocean after the Fukushima accident and analysis of its dispersion in Japanese coastal waters. J. Geophys. Res. 117, C11014. http://dx.doi.org/10.1029/2012JC007933.

Evangeliou, N., Balkanski, Y., Cozic, A., Møller, A.P., 2014. Global and local cancer risks after the Fukushima Nuclear Power Plant accident as from Chernobyl: a modeling study for radiocaesium (^{134}Cs & ^{137}Cs). Environ. Internal. 64, 17–27.

Evrard, O., Van Beek, P., Gateuille, D., Pont, V., Lefevre, I., Lansard, B., et al., 2012. Evidence of the Radioactive Fallout in France Due to the Fukushima Nuclear Accident 114, pp. 54–60.

Furuta, S., Sumiya, S., Watanabe, H., Nakano, M., Imaizumi, K., Takeyasu, M., et al., 2011. Results of the environmental radiation monitoring following the accident at the Fukushima Daiichi nuclear power plant – interim report (ambient radiation dose rate, radioactivity concentration in the air and radioactivity concentration in the fallout). JAEA-Rev. 2011-035, p. 1–84 (In Japanese).

Garcia, F.P., Garcia-Ferro, M.A., 2012. Traces of fission products in southeast Spain after the Fukushima nuclear accident. J. Environ. Radioact. 109, 13–18.

Glavic-Cindro, D., Benedik, L., Kožar Logar, J., Vodenik, B., Zorko, B., 2013. Detection of Fukushima plume within regular Slovenian environmental radioactivity surveillance. Appl. Radiat. Isot. 81, 374–378.

Haba, H., Kanaya, J., Mukai, H., Kambara, T., Kase, M., 2012. One-year monitoring of airborne radionuclides in Wako, Japan, after the Fukushima Dai-ichi nuclear power plant accident in 2011. Geochem. J. 46, 271–278.

Hamada, N., Ogino, H., 2012. Food safety regulations: what we learned from the Fukushima nuclear accident. J. Environ. Radioact. 111, 83–99.

Hardie, S.M.L., McKinley, I.G., 2014. Fukushima remediation: status and overview of future plans. J. Environ. Radioact. 133, 75–85.

Hirao, S., Yamazawa, H., Nagae, T., 2013. Estimation of release rate of Iodine-131 and cesium-137 from the Fukushima Daiichi nuclear plant. J. Nucl. Sci. Technol. 50, 139–147.

Hirose, K., 2012. 2011 Fukushima Daiichi nuclear power plant accident: summary of regional radioactivity deposition monitoring results. J. Environ. Radioact. 111, 13–17.

Hirose, K., 2013. Temporal variation of monthly ^{137}Cs deposition observed in Japan: effects of the Fukushima Daiichi nuclear power plant accident. Appl. Radiat. Isot. 66, 1675–1678.

Hirose, K., 2015a. Two-years trend of monthly ^{137}Cs deposition observed in Kanto and south Tohoku areas, Japan: effects of the Fukushima Dai-ichi nuclear power plant accident. J. Radioanal. Nucl. Chem. 303, 1327–1329.

Hirose, K., 2015b. Current trends of ^{137}Cs concentrations in coastal waters near the Fukushima Daiichi NPP. J. Radioanal. Nucl. Chem. http://dx.doi.org/10.1007/s10967-015-4537-z.

Hirose, K., Igarashi, Y., Aoyama, M., 2008. Analysis of 50 years records of atmospheric deposition of long-lived radionuclides in Japan. Appl. Radiat. Isot. 66, 1675–1678.

Högberg, L., 2013. Root causes and impacts of severe accidents at large nuclear power plants. Ambio 42, 267–284.
Honda, M.C., Kawakami, H., 2014. Sinking velocity of particulate radiocesium in the northwestern North Pacific. Geophys. Res. Lett. http://dx.doi.org/10.1002/2014GL060126.
Honda, M.C., Aono, T., Aoyama, M., Hamajima, Y., Kawakami, H., Kitamura, M., Matsumoto, Y., Miyazawa, Y., Takigawa, M., Saino, T., 2012. Dispersion of artificial caesium-134 and -137 in the western North Pacific onemonth after the Fukushima accident. Geochem. J. 45, e1–e9.
Honda, M.C., Kawakami, H., Watanabe, S., Saino, T., 2013. Concentrations and vertical flux of Fukushima-derived radiocesium in sinking particles from two sites in the Northwestern Pacific Ocean. Biogeosciences 10, 3525–3534.
Hou, X., Povinec, P.P., Zhang, L., Shi, K., Biddulph, D., Chang, C.-C., et al., 2013. Iodine-129 in seawater offshore Fukushima: distribution, inorganic speciation, sources and budget. Environ. Sci. Technol. 47, 3091–3098.
Hsu, S.C., Huh, C.A., Chan, C.Y., Lin, S.H., Lin, F.J., Liu, S.C., 2012. Hemispheric dispersion of radioactive plume laced with fission nuclides from the Fukushima nuclear event. Geophys. Res. Lett. 39, L00G22.
Huh, C.A., Hsu, S.-C., Lin, C.-Y., 2012. Fukushima-derived fission nuclides monitored around Taiwan: free tropospheric versus boundary layer transport. Earth Planet. Sci. Lett. 319–320, 9–14.
Igarashi, Y., Kajino, M., Zaizen, Y., Adachi, K., Mikami, M., 2015. Atmospheric radioactivity over Tsukuba, Japan: a summary of three years of observations after the FDNPP accident. Prog. Earth Planet. Sci. 2, 44. http://dx.doi.org/10.1189/s40645 -015-0066-1.
Inomata, Y., Aoyama, M., Tsumune, D., Tsubono, T., Hirose, K., Torii, T., Sanada, Y., Yamada, Y., 2014. Distribution of radioactive materials in the surface sea water developed by aerial radiological survey. J. Nucl. Sci. Tech. 51, 1059–1063.
Inomata, Y., Aoyama, M., Tsubono, T., Tsumune, D., Hirose, K., 2016. Spatial and temporal distribution of ^{134}Cs and ^{137}Cs derived from TEPCO Fukushima Daiichi Nuclear Power Plant accident into the North Pacific Ocean by using optimal interpolation analysis. Environ. Sci. Process. Impacts. http://dx.doi.org/10.1039/C5EM00324E.
Inoue, M., Kofuji, H., Nagao, S., Yamamoto, M., Hamajima, Y., Yoshida, K., Fujimoto, K., Takada, T., Isoda, Y., 2012a. Lateral variation of ^{134}Cs and ^{137}Cs concentrations in surface seawater in and around the Japan sea after the Fukushima Dai-ichi Nuclear Power Plant accident. J. Environ. Radioact. 109, 45–51.
Inoue, M., Kofuji, H., Hamajima, Y., Nagao, S., Yoshida, K., Yamamoto, M., 2012b. ^{134}Cs and ^{137}Cs activities in coastal seawater along Northern Sanriku and Tsugaru Strait, northeaster Japan, after Fukushima Dai-ichi Nuclear Power Plant accident. J. Environ. Radioact. 111, 116–119.
Inoue, M., Kofuji, H., Nagao, S., Yoshida, K., Yamamoto, M., Hamajima, Y., Fujimoto, K., Yoshida, K., Suzuki, A., Takashiro, H., Hayakawa, K., Hamataka, K., Yoshida, S., Kunugi, M., Minakawa, M., 2012c. Low levels of ^{134}Cs and ^{137}Cs in surface seawaters around the Japanese Archipelago after the Fukushima Dai-ichi Nuclear Power Plant accident in 2011. Geochem. J. 46, 311–320.
Kaeriyama, H., Ambe, D., Shimizu, Y., Fujimoto, K., Ono, T., Yonezaki, S., Kato, Y., Matsunaga, H., Minami, H., Nakatsuka, S., Watanabe, T., 2013. Direct observation of ^{134}Cs and ^{137}Cs in surface seawater in the western and central North Pacific after the Fukushima Dai-ichi Nuclear Poser Plant accident. Biogeosciences 10, 4287–4295.
Kaeriyama, H., Shimizu, Y., Ambe, D., Masujima, M., Shigenobu, Y., et al., 2014. Southwest intrusion of ^{134}Cs and ^{137}Cs derived from the Fukushima Dai-ichi Nuclear Power Plant accident in the Western North Pacific. Environ. Sci. Technol. 48, 3120–3127.
Kameník, J., Dulaiova, H., Buesseler, K.O., Pike, S.M., Šťastna, K., 2013. Cesium-134 and 137 activities in the central North Pacific Ocean after the Fukushima Dai-ichi Nuclear Power Plant accident. Biogeoscience 10, 6045–6052.
Kanai, Y., 2012. Monitoring of aerosols in Tsukuba after Fukushima Nuclar Power Plant incident in 2011. J. Environ. Radioact. 111, 33–37. http://dx.doi.org/10.1016/j.jenvrad.2011.10.011.
Kanai, Y., Doi, T., Masumoto, K., 2013. Observation of radionuclides transported with aerosols at the GSJ in 2012 and re-examination of meteorological factors. Bull. Geol. Surv. Jpn. 64, 139–150 (in Japanese).
Kanda, J., 2013. Continuing ^{137}Cs release to the sea from the Fukushima Dai-ichi nuclear power plant through 2012. Biogeosciences 10, 6103–6113.
Kaneyasu, N., Ohashi, H., Suzuki, F., Okuda, T., Ikemori, F., 2012. Sulfate aerosol as a potential transport medium of radiocesium from the Fukushima nuclear accident. Environ. Sci. Technol. 46, 5720–5726.
Kashparov, V.A., Lundin, S.M., Zvarych, S.I., Yoshchenko, V.I., Levchuk, S.E., Khomutinin, V.Y., et al., 2003. Territory contamination with the radionuclides representing the fuel component of Chernobyl fallout. Sci. Total Environ. 317, 105–119.
Katata, G., Ota, M., Terada, H., Chino, M., Nagai, H., 2012. Atmospheric discharge and dispersion of radionuclides during the Fukushima Dai-ichi nuclear power plant accident. Part I: source term estimation and local-scale atmospheric dispersion in early phase of the accident. J. Environ. Radioact. 109, 103–113.
Katata, G., Chino, M., Kobayashi, T., Terada, H., Ota, M., Nagai, H., Kajino, M., Draxier, R., Hort, M.C., Malo, A., Torii, T., Sanada, Y., 2015. Detailed source term estimation of the atmospheric release for the Fukushima Daiichi nuclear power station accident by coupling simulations of atmospheric dispersion model with improved deposition scheme and oceanic dispersion model. Atmos. Chem. Phys. 15, 1029–1070.
Kawamura, H., Kobayashi, T., Furuno, A., In, T., Ishikawa, Y., Nakayama, T., Shima, S., Awaji, T., 2011. Preliminary numerical experiments on oceanic dispersion of ^{131}I and ^{137}Cs discharged into the ocean because of the Fukushima Daiichi Nuclear Power Plant disaster. J. Nucl. Sci. Technol. 48, 1349–1356.
Kawamura, H., Kobayashi, T., Furuno, A., Usui, N., Kamachi, M., 2014. Numerical simulation on the long-term variation of radioactive cesium concentration in the North Pacific due to the Fukushima disaster. J. Environ. Radioact. 136, 64–75.
Kim, C.-K., Byun, J.-I., Chae, J.-S., Choi, H.-Y., Choi, S.-W., Kim, D.-J., et al., 2012. Radiological impact in Korea following the Fukushima nuclear accident. J. Environ. Radioact. 111, 70–82.
Kinoshita, N., Sueki, K., Sasa, A., Kitagawa, J., Ikarashi, S., Nishimura, T., Wong, Y.S., Satou, Y., Handa, K., Takahashi, T., Sato, M., Yamagata, T., 2011. Assessment of individual radionuclide distributions from the Fukushima nuclear accident covering central-east Japan. Proc. Natl. Acad. Sci. 108 (49), 19526–19529.
Kitto, M.E., Menia, T.A., Hains, D.K., Beach, S.E., Bradt, C.J., Fielman, E.M., et al., 2013. Airborne gamma-ray emitters from Fukushima detected in New York State. J. Radioanal. Nucl. Chem. 296, 49–56.
Kobayashi, T., Nagai, H., Chino, M., Kawamura, H., 2013. Source term estimation of atmospheric release due to the Fukushima Dai-ichi Nuclear Power Plant accident by atmospheric and ocean simulations. J. Nucl. Sci. Technol. 50, 255–264.
Kofuji, H., Inoue, M., 2013. Temporal variations in ^{134}Cs and ^{137}Cs concentrations in seawater along the Shimokita Peninsula and the northern Sanriku coast in northeastern Japan, one year after the Fukushima Dai-ichi Nuclear Power Plant accident. J. Environ. Radioact. 124, 239–245.
Koo, Y.-H., Yang, Y.-S., Song, K.-K., 2014. Radioactivity release from the Fukushima accident and its consequences: a review. Prog. Nucl. Energy 74, 61–70.
Korsakissok, I., Mathieu, S., Didier, D., 2013. Atmospheric dispersion and ground deposition induced by the Fukushima Nuclear Power Plant accident: a local-scale simulation and sensitivity study. Atmos. Environ. 70, 267–279.
Kritidis, P., Florou, H., Eleftheriadis, K., Evangeliou, N., Gini, M., Sotiropoulou, M., et al., 2012. Radioactive pollution in Athens, Greece due to the Fukushima nuclear accident. J. Environ. Radioact. 114, 100–104.
Kumamoto, Y., Aoyama, M., Hamajima, Y., Aono, T., Kouketsu, S., Murata, A., Kawano, T., 2014. Southward spreading of the Fukushima-derived radiocesium across the Kuroshio Extension in the North Pacific. Sci. Rep. 4, 4276. http://dx.doi.org/10.1038/srep04276.
Kumamoto, Y., Murata, A., Kawano, T., Aoyama, M., 2013. Fukushima-derived radiocesium in the northwestern Pacific Ocean. Appl. Radiat. Isoto. 81, 335–339.
Le Petit, G., Douysset, G., Ducros, G., Gross, P., Achim, P., Monfort, M., Raymond, P., Pontillon, Y., Jutier, C., Blanchard, X., 2014. Analysis of radionuclide releases from the Fukushima Dai-Ichi nuclear power plant accident Part I. Pure Appl. Geophys. 171, 629–644.
Loaiza, P., Brudanin, V., Piquemal, F., Reyss, J.-L., Stekl, I., Warot, G., et al., 2012. Air radioactivity levels following the Fukushima reactor accident measured at the Laboratoire Souterrain de Modane, France. J. Environ. Radioact. 114, 66–70.
Long, N.Q., Truong, Y., Hien, P.D., Binh, N.T., Sieu, L.N., Giap, T.V., Phan, N.T., 2012. Atmospheric radionuclides from the Fukushima Dai-ichi nuclear reactor accident observed in Vietnam. J. Environ. Radioact. 111, 53–58. http://dx.doi.org/10.1016/j.jenvrad.2011.11.018.
Lou Brandon, 2012. NRC Protective Measures Team Fukushima Challenges; RASCAL 4.2 Update. National Radiological Emergency Preparedness Conference, USNRC.
Lozano, R.L., Hernández-Ceballos, M.A., Adame, J.A., Casas-Ruíz, M., Sorribas, M., San Miguel, E.G., Bolívar, J.P., 2011. Radioactive impact of Fukushima accident on the Iberian Peninsula: evolution and plume previous pathway. Environ. Int. 37, 1259–1264.
Lujanienė, G., Bycenkienė, S., Povinec, P.P., Gera, M., 2012. Radionuclides from the Fukushima accident in the air over Lithuania: measurement and modeling approaches. J. Environ. Radioact. 114, 71–80. http://dx.doi.org/10.1016/j.jenvrad.2011.12.004.
Lyons, C., Colton, D., 2012. Aerial measuring system in Japan. Health Phys. 102, 509–515.
MacMullin, S., Giovanetti, G.K., Green, M.P., Henning, R., Holmes, R., Vorren, K., et al., 2012. Measurement of airborne fission products in Chapel Hill, NC, USA from the Fukushima nuclear accident. J. Environ. Radioact. 112, 165–170.
Manolopoulou, M., Vagena, E., Syoulos, S., Loannidou, A., Papastefanou, C., 2011. Radioiodine and radiocesium in Thessaloniki, Greece due to the Fukushima nuclear accident. J. Environ. Radioact. 102, 796–797.
Marzo, G.A., 2014. Atmospheric transport and deposition of radionuclides released after the Fukushima Dai-ichi accident and resulting effective dose. Atmos. Environ. 94, 709–722.
Masson, O., Baeza, A., Bieringer, J., Brudecki, K., Bucchi, S., Cappai, M., et al., 2011. Tracking of airborne radionuclides from the damaged Fukushima Dai-ichi nuclear reactors by European networks. Environ. Sci. Technol. 45, 7670–7677.
Masson, O., Ringer, W., Malá, H., Rulik, P., Dlugosz-Lisiecka, M., Eleftherisdis, K., Meisenberg, O., De Vismes-Ott, A., Gensdarmes, F., 2013. Size distributions of airborne radionuclides from the Fukushima nuclear accident at several places on Europe. Environ. Sci. Technol. 47, 10995–11003.
Masumoto, Y., Miyazawa, Y., Tsumune, D., Tsubono, T., Kobayashi, T., Kawamura, H., Estournel, C., Marselexis, P., Lanerolle, L., Mehra, A., Garraffo, Z.D., 2012. Oceanic dispersion simulations of ^{137}Cs released from the Fukushima Daiichi nuclear power plant. Elements 8, 207–212.
McNaughton, M., 2011. Los Alamos air Monitoring Data Related to the Fukushima Daiichi Reactor. LA-UR-11-10304.
Men, W., He, J., Wang, F., Wen, F., Li, Y., Huang, J., Yu, X., 2014. Radioactive status of seawater in the northwest Pacific more than one year after the Fukushima

nuclear accident. Sci. Rep. 5, 7757. http://dx.doi.org/10.1038/srep07757.
MEP, Ministry Environmental Protection, 2011. The People's Republic of China. http://english.mep.gov.cn/news_service/news_release/201103/t20110330_208126.htm.
Mikami, S., Maeyama, T., Hoside, Y., Sakamoto, Y., Sato, S., Okuda, N., Demongeot, S., Gurriaran, R., Uwamino, Y., Kato, H., Fujiwara, M., Sato, T., Takemiya, H., Saito, K., 2015. Spatial distributions of radionuclides deposited onto ground soil around the Fukushima Dai-ichi Nuclear Power Plant and their temporal change until December 2012. J. Environ. Radioact. 139, 320–343.
Miley, H.S., Bowyer, T.W., Engelmann, M.D., Eslinger, P.W., Friese, J.A., Greenwood, L.R., et al., 2013. Measurement of Fukushima aerosol debris in Sequim and Richland, WA and Ketchikan, AK. J. Radioanal. Nucl. Chem. 296, 877–882.
Min, B.-I., Perianeez, R., Kim, I.-G., Suh, K.-S., 2013. Marine dispersion assessment of ^{137}Cs released from the Fukushima nuclear accident. Mar. Poll. Bull.
Miyake, Y., Matsuzaki, H., Fujiwara, T., Saito, T., Yamagata, T., Honda, M., Muramatsu, Y., 2012. Isotopic ratio of radioactive iodine (^{129}I/^{131}I) released from Fukushima Daiichi NPP accident. Geochem. J. 46 (4), 327–333.
Miyazawa, Y., Masumoto, Y., Varlamov, S.M., Miyama, T., 2012. Transport simulation of the radionuclide from the shelf to open ocean around Fukushima. Cont. Shelf Res. 50–51, 16–29.
Miyazawa, Y., Masumoto, Y., Varlamov, S.M., Miyama, T., Takigawa, M., Honda, M., Saino, T., 2013. Inverse estimation of source parameters of oceanic radioactivity dispersion models associated with the Fukushima accident. Biogeosciences 10, 2349–2363.
Momoshima, N., Sugihara, S., Ichikawa, R., Yokoyama, H., 2012. Atmospheric radionuclides transported to Fukuoka, Japan remote from the Fukushima Dai-ichi nuclear power complex following the nuclear accident. J. Environ. Radioact. 111, 28–32.
Morino, Y., Ohara, T., Nishizawa, M., 2011. Atmospheric behavior, deposition, and budget of radioactive materials from the Fukushima Daiichi nuclear power plant in March 2011. Geophys. Res. Lett. 38. L00G11.
Muramatsu, Y., Matsuzaki, H., Toyama, C., Ohno, T., 2015. Analysis of ^{129}I in the soils of Fukushima prefecture: preliminary reconstruction of ^{131}I deposition related to the accident at Fukushima Daiichi Nuclear Power Plant (FDNPP). J. Environ. Radioact. 139, 344–350.
Nakano, M., Povinec, P.P., 2012. Long-term simulations of ^{137}Cs dispersion from the Fukushima accident in the world ocean. J. Environ. Radioact. 111, 109–115.
Nakano, H., Motoi, T., Hirose, K., Aoyama, M., 2010. Analysis of ^{137}Cs concentration in the Pacific using a Lagrangian approach. J. Geophys. Res. 115. C06015.
Nakata, K., Sugisaki, H., 2015. Impacts of the Fukushima Nuclear Accident on Fish and Fishing Grounds. FRA, Springer Open. http://dx.doi.org/10.1007/978-4-431-55537-7.
Nikolic, J., Pantelic, G., Todorovic, D., Jankovic, M., Savkovic, M.E., 2012. Monitoring of aerosol and fallout radioactivity in Belgrade after the Fukushima reactors accident. Water Air Soil Pollut. 223, 4823–4829.
Oikawa, S., Takata, H., Watabe, T., Misonoo, J., Kusakabe, M., 2013. Distribution of the Fukushima-derived radionuclides in seawater in the Pacific off the coast of Miyagi, Fukushima, and Ibaraki Prefectures, Japan. Biogeosciences 10, 5031–5047.
Onda, Y., Kato, H., Hoshi, M., Yakahashi, Y., Nguyen, M.L., 2015. Soil sampling and analytical strategies for mapping fallout in nuclear emergencies based on the Fukushima Dai-ichi nuclear power plant accident. J. Environ. Radioact. 139, 300–307.
Paatero, J., Vira, J., Siitari-Kauppi, M., Hatakka, J., Holmen, K., Viisanen, Y., 2012. Airborne fission products in the high Arctic after the Fukushima nuclear accident. J. Environ. Radioact. 114, 41–47. http://dx.doi.org/10.1016/j.jenvrad.2011.12.027.
Parache, V., Pourcelot, L., Roussel-Debet, S., Orjollet, D., Leblanc, F., Soria, C., et al., 2011. Transfer of ^{131}I from Fukushima to the vegetation and milk in France. Environ. Sci. Technol. 45, 9998–10003.
Periáñez, R., Suh, K.-S., Min, B.-I., 2012. Local scale marine modelling of Fukushima releases. Assessment of water and sediment contamination and sensitivity to water circulation description. Mar. Poll. Bull. 64, 2333–2339.
Periáñez, R., Brovchenko, I., Duffa, C., Jung, K.-T., Kobayashi, T., Lamego, F., Maderich, V., Min, B.-I., Nies, H., Osvath, I., Psaltaki, M., Suh, K.-S., 2015. A new comparison of marine dispersion model performances for Fukushima Dai-ichi releases in the frame of IAEA MODARIA program. J. Environ. Radioact. 150, 247–269.
Pham, M.K., Eriksson, M., Levy, I., Nies, H., Osvath, I., Betti, M., 2012. Detection of Fukushima Daiichi nuclear power plant accident radioactive tracers in Monaco. J. Environ. Radioact. 114, 131–137.
Pittauerová, D., Hettwig, B., Fischer, H.W., 2011. Fukushima fallout in Northwest German environmental media. J. Environ. Radioact. 102, 877–880.
Povinec, P.P., Hirose, K., 2015. Fukushima radionuclides in the NW Pacific, and assessment of doses for Japanese and world population from ingestion of seafood. Sci. Rep. 5, 9016. http://dx.doi.org/10.1038/srep09016.
Povinec, P.P., Hirose, K., Aoyama, M., 2012a. Radiostrotium in the western North Pacific: characteristics, behavior and the Fukushima impact. Environ. Sci. Technol. 46, 10356–10363.
Povinec, P.P., Sykora, I., Holý, K., Gera, M., Kovacik, A., Brestakova, L., 2012b. Aerosol radioactivity record in Bratislava/Slovakia following the Fukushima accident. J. Environ. Radioact. 114, 81–88.
Povinec, P.P., Hirose, K., Aoyama, M., 2013a. Fukushima Accident: Radioactivity Impact on the Environment. Elsevier, New York.
Povinec, P.P., Aoyama, M., Biddulph, D., Breier, R., Busseler, K., Chang, C.C., Golser, R., Hou, X.L., Ješkovský, M., Jull, A.J.T., Kaizer, J., Nakano, M., Nies, H., Palcsu, L., Pham, M.K., Steier, P., Zhang, L.Y., 2013b. Cesium, iodine and tritium in NW Pacific waters – a comparison of eh Fukushima impact with global fallout. Biogeosciences 10, 5481–5496.
Povinec, P.P., Gera, M., Holý, K., Hirose, K., Lujaniené, G., Nakano, M., Plastino, W., Sýkora, I., Bartok, J., Gažák, M., 2013c. Dispersion of Fukushima radionuclides in the global atmosphere and the ocean. Appl. Radiat. Isot. 81, 383–392.
Ramzaev, V., Barkovsky, A., Goncharova, Yu, Gromov, A., Kaduka, M., Romanovich, I., 2013. Radiocesium fallout in the grasslands on Sakhalin, Kunashir and Shikotan Islands due to Fukushima accident: radioactive contamination of soil and plants in 2011. J. Environ. Radioact. 118, 128–142.
Ramzaev, V., Nikitin, A., Sevastyanov, A., Artemiev, G., Bruk, G., Ivanov, S., 2014. Shipboard determination of radiocesium in seawater after the Fukushima accident: results from the 2011–2012 Russian expeditions to the Sea of Japan and western North Pacific Ocean. J. Environ. Radioact. 135, 13–24.
Rizzo, S., Tomarchio, E., 2012. Radionuclides concentrations in air particulate at Palermo (Italy) following Fukushima accident. Radiat. Prot. Dosim. http://dx.doi.org/10.1093/rpd/ncs120.
Rossi, V., Van Sebille, E., Gupta, A.S., Garçon, V., Engalnd, M.H., 2013. Multi-decadal projections of surface and interior pathways of Fukushima Cesium-137 radioactive plume. Deep-Sea Res. I 80, 37–46.
Rossi, V., Van Sebille, E., Gupta, A.S., Garçon, V., Engalnd, M.H., 2014. Corrigendum to multi–decadal projections of surface and interior pathways of Fukushima Cesium-137 radioactive plume. Deep-Sea Res. I 93, 162–164.
Rypina, I.I., Jayne, S.R., Yoshida, S., Macdonald, A.M., Douglass, E., Buesseler, K., 2013. Short-term dispersal of Fukushima-derived radionuclides off Japan: modeling efforts and model-data intercomparison. Biogeosciences 10, 4973–2990.
Saito, K., Shimbori, T., Draxler, R., 2015a. JAM's regional atmospheric transport model calculations for the WMO technical task team on meteorological analyses for Fukushima Daiichi Nuclear Power Plant accident. J. Environ. Radioact. 139, 185–199.
Saito, K., Tanihata, I., Fujiwara, M., Saito, T., Shimoura, S., Otsuka, T., Onda, Y., Hoshi, M., Ikeuchi, Y., Takahashi, F., Kinouchi, N., Saegusa, J., Seki, A., Takamiya, H., Shibata, T., 2015b. Detailed deposition density maps constructed by large-scale soil sampling for gamma-emitting radioactive nuclides from the Fukushima Dai-ichi Nuclear Power Plant accident. J. Environ. Radioact. 139, 308–319.
Sakaguchi, A., Steiner, P., Takahashi, Y., Yamamoto, M., 2014. Isotopic compositions of ^{236}U and Pu isotopes in "Black Substances" collected from roadsides in Fukushima Prefecture: Fallout from the Fukushima Dai-ichi Nuclear Power Plant accident. Environ. Sci. Technol. 78, 3691–3697.
Sanada, Y., Sugita, T., Nishizawa, Y., Kondo, A., Torii, T., 2014. The aerial radiation monitoring in Japan after the Fukushima Daiichi nuclear power plant accident. Proc. Nucl. Sci. Tech. 4, 76–80.
Saunier, O., Mathieu, A., Didier, D., Tombette, M., Quelo, D., Winiarek, V., Bocquet, M., 2013. An inverse modeling method to assess the source term of the Fukushima Nuclear Power Plant accident using gamma dose rate observations. Atmos. Chem. Phys. 13, 11403–11421.
Schöppner, M., Plastino, W., Povinec, P.P., Watowa, G., Bella, F., Budano, A., De Vincenzi, M., Ruggieri, F., 2012. Estimation of the time-dependent radioactive source-term from the Fukushima nuclear power plant accident using atmospheric transport modelling. J. Environ. Radioact. 114, 10–14.
Schöppner, M., Plastino, W., Povinec, P.P., Nikkinen, M., Ruggieri, F., Bella, F., 2013. Estimation of the radioactive source dispersion from the Fukushima nuclear power plant accident. Appl. Radiat. Isot. 81, 358–361.
SCJ, 2014. A Review of the Model Comparison of Transportation and Deposition of Radioactive Materials Released to the Environment as a Result of the Tokyo Electric Power Company's Fukushima Daiichi Nuclear Power Plant Accident. Sectional Committee on Nuclear Accident, Committee on Comprehensive Synthetic Engineering, Science Council of Japan.
Smith, J.N., Brown, R.M., Williams, W.J., Robert, M., Nelson, R., Moran, S.B., 2015. Arrival of the Fukushima radioactivity plume in North American continental waters. Proc. Natl. Acad. Sci. U. S. A. 112, 1310–1315.
Srinivas, C.V., Venkatesan, R., Baskaran, R., Rajagopal, V., Venkatraman, B., 2012. Regional scale atmospheric dispersion simulation of accidental releases of radionuclides from Fukushima Dai-ichi reactor. Atmos. Environ. 61, 66–84.
Steinhauser, G., Brandl, A., Johnson, T.E., 2014. Comparison of the Chernobyl and Fukushima nuclear accidents: a review of the environmental impacts. Sci. Total Environ. 470–471, 800–817.
Steinhauser, G., Niisoe, T., Harada, K.H., Shozugawa, K., Schneider, S., Synal, H.-A., Walther, C., Christl, M., Nanba, K., Ishikawa, H., Koizumi, A., 2015. Post-accident sporadic release of airborne radionuclides from the Fukushima Daiichi Nuclear Power Plant site. Environ. Sci. Technol. 49, 14028–14035.
Stohl, A., Selbert, P., Watowa, G., Arnord, D., Burkhart, J.F., Eckhardt, S., Tapia, C., Vargas, A., Yasunari, T.J., 2012. Xenon-133 and caesium-137 releases into the atmosphere from the Fukushima Dai-ichi nuclear power plant: determination of the source term, atmospheric dispersion, and deposition. Atmos. Chem. Phys. 12, 2313–2343.
Sugiyama, G., Nasstrom, J., Pobanz, B., Foster, K., Simpson, M., Vogt, P., Aluzzi, F., Homann, S., 2012. Atmospheric dispersion modeling: challenges of the Fukushima Daiichi response. Health Phys. 102, 493–508.
Takemura, T., Nakamura, H., Takigawa, M., Kondo, H., Satomura, T., Miyasaka, T., Nakajima, T., 2011. A numerical simulation of global transport of atmospheric particles emitted from the Fukushima Daiichi Nuclear Power Plant. Sora 7,

101–104.
Tateda, Y., Tsumune, D., Tsubono, T., Aono, T., Kanda, J., Ishimaru, T., 2015. Radiocesium biokinetics in olive flounder inhabiting the Fukushima-accident affected Pacific coastal waters of eastern Japan. J. Environ. Radioact. 147, 131–141.
Ten Hoeve, J.E., Jacobson, M.Z., 2012. Worldwide health effects of the Fukushima Daiichi nuclear accident. Energ. Environ. Sci. 5, 8743–8757.
Terada, H., Katada, G., Chino, M., Nagai, H., 2012. Atmospheric discharge and dispersion of radionuclides during the Fukushima Daiichi nuclear power plant accident. Part II: verification of the source term and analysis of regional-scale atmospheric dispersion. J. Environ. Radioact. 112, 141–154.
Thakur, P., Ballard, S., Nelson, R., 2013. An overview of Fukushima radionuclide measured in the northern hemisphere. Sci. Total Environ. 458–460, 577–613.
Tsumune, D., Aoyama, M., Hirose, K., 2003. Behavior of ^{137}Cs concentrations in North Pacific in an ocean general circulation model. J. Geophys. Res. 108 (C8), 3262.
Tsumune, D., Tsubono, T., Aoyama, M., Hirose, K., 2012. Distribution of oceanic ^{137}Cs from the Fukushima Daiichi Nuclear Power Plant simulated numerically by a regional ocean model. J. Environ. Radioact. 111, 100–108.
Tsumune, D., Tsubono, T., Aoyama, M., Uematsu, M., Misumi, K., Maeda, Y., Yoshida, Y., Hayami, H., 2013. One-year, regional-scale simulation of ^{137}Cs radioactivity in the ocean following the Fukushima Dai-ichi Nuclear Power Plant accident. Biogeosciences 10, 5601–5617.
Tsuruta, H., Oura, Y., Ebihara, M., Ohara, T., Nakajima, T., 2014. First retrieval of hourly atmospheric radionuclides just after the Fukushima accident by analyzing filter-tapes of operational air pollution monitoring stations. Sci. Rep. 4, 6717.
UNSCEAR, 2008. Sources and Effects of Ionizing Radiation (Annex D) New York: United Nation.
UNSCEAR, 2013. Sources and Effects of Ionizing Radiation (Annex A) New York: United Nation.
US-EPA (United States Environmental Protection Agency), 2011. http://www.epa.gov/japan2011/rert/RadNet-sampling-data.html.
USNRC, 2012. State-of-the-art Reactor Consequence Analysis Report. U.S.NRC, Washington, DC. Report NUREG-1935.
Wada, T., Nemoto, Y., Shimamura, S., Fujita, T., Mizuno, T., Sohtome, T., Kamiyama, K., Morita, T., Igarashi, S., 2013. Effects of the nuclear disaster on marine products in Fukushima. J. Environ. Radioact. 124, 246–254.
Winiarek, V., Bocquet, M., Saunier, O., Mathieu, A., 2012. Estimation of errors in the inverse modeling of accidental release of atmospheric pollutant; application to the reconstruction of the cesium-137 and iodine-131 source terms from the Fukushima Daiichi power plant. J. Geophys. Res. 117. D05122/1–16.
Winiarek, V., Bocquet, M., Duhanyan, N., Roustan, Y., Saunier, O., Mathieu, A., 2014. Estimation of the caesium-137 source term from the Fukushima Daiichi nuclear power plant using a consistent joint assimilation of air concentration and deposition observations. Atmos. Environ. 82, 268–279.
Yamamoto, M., Sakaguchi, A., Ochiai, S., Takeda, T., Hamataka, K., Murakami, T., Nagao, S., 2014. Isotopic Pu, Am and Cm signatures in environmental samples contaminated by the Fukushima Dai-ichi Nuclear Power Plant accident. J. Environ. Radioact. 132, 31–46.
Yasunari, T.J., Dtohl, A., Hayano, R.S., Burkhalt, J.F., Eckhardt, S., Yasunari, T., 2011. Cesium-137 deposition and contamination of Japanese soils due to the Fukushima nuclear accident. Proc. Natl. Acad. Sci. U. S. A. 108, 19530–19580.
Yonezawa, C., Yamamoto, Y., 2011. Measurements of Artificial Radionuclides in Surface Air by CTBTO Network, Bunseki, pp. 451–458 (in Japanese).
Yoshida, N., Takahashi, Y., 2012. Land-surface contamination by radionuclides from the Fukushima Daiichi Nuclear Power Plant accident. Elements 8, 201–206.
Yoshida, S., Macdonald, A.M., Jayne, S.R., Rypina, I.I., Buesseler, K.O., 2015. Observed eastwars progression of the Fukushima ^{134}Cs signal across the North Pacific. Geophys. Res. Lett. 42, 7139–7142.
Yu, W., He, J., Lin, W., Li, Y., Men, W., Wang, F., 2015. Distribution and risk assessment of radionuclides released by Fukushima nuclear accident at the northwest Pacific. J. Environ. Radioact. 142, 54–61.
Zhang, W., Bean, M., Benotto, M., Cheung, J., Ungar, K., Ahier, B., 2011. Development of a new aerosol monitoring system and its application in Fukushima nuclear accident related aerosol radioactivity measurement at the CTBT radionuclide station in Sidney of Canada. J. Environ. Radioact. 102, 1065–1069.
Zheng, J., Tagami, K., Watanabe, Y., Uchida, S., Aono, T., Ishii, N., Yoshida, S., Kubota, Y., Fuma, S., Ihara, S., 2012. Isotopic evidence of plutonium release into the environment from the Fukushima DNPP accident. Sci. Rep. 2, 304. http://dx.doi.org/10.1038/step00304.